TABLE OF CONTENTS

List of Tables

List of Figures

2.5.METEOROLOGY

2.5.1. *Introduction*

Meteorological data have been compiled for ten sites surrounding the proposed Ludeman Project area. Data were acquired through the Western Regional Climate Center (WRCC, 2007) for eight Cooperative Observer Program (COOP) and Automated Surface Observation Stations (ASOS) stations operated by the National Weather Service (NWS) including Casper Airport, Douglas AP (AP), Dull Center 1SE, Glenrock 5 ESE, Kaycee, Lance Creek 3 WNW, Midwest, and Reno. Hourly data were obtained for Casper and Douglas (NCDC 2015). In addition, Glenrock Coal Company (GCC) and Antelope Coal Company (ACC) meteorological data have been obtained through Inter-Mountain Laboratories (IML). On-site data have been obtained from the Ludeman Project meteorological station, owned by Uranium One Americas and operated by IML. The GCC, ACC and Ludeman sites are operated in compliance with regulations set forth by the Wyoming Air Quality Division (AQD) for air quality monitoring. Table 2.5-1 provides the station id, coordinates (UTM metric, Zone 13, NAD 27), elevation, and period of record for all of the meteorological stations used in this study. Hourly wind data for Casper were taken from 1997 through 2014. Hourly wind data for Douglas were taken from 2003 through 2014.

Ten of these 11 sites have been analyzed collectively to provide a regional climatic temperature and precipitation analysis that includes the proposed project area. The Casper, Douglas, and GCC sites were analyzed for the regional wind summaries. The eight NWS sites have been incorporated into the snowfall analysis. One year of meteorological data from the proposed Ludeman Project site was utilized for the on-site discussion.

A regional overview is presented first. This section includes a discussion of the maximum and minimum temperature, relative humidity, annual precipitation including snowfall estimates, and a brief wind speed and direction summary. The last portion of the regional analysis includes a general climate data summary from Casper.

A site specific analysis follows the regional overview. This analysis is based on the baseline year of on-site meteorological data, with many of the same meteorological parameters listed previously. An in-depth wind analysis summarizes average wind speeds and directions, wind roses, wind speed frequency distributions, and a joint frequency distribution to characterize the wind data for the Ludeman Project site by stability class. A

monthly or seasonal data analysis is included for the temperature and wind parameters. The seasonal classification does not coincide with official calendar seasons; rather, it uses three-month intervals as follows; January – March for winter, April-June for spring, July – September for summer, and October – December for fall. Beyond wind and temperature data, general climate data from the regional evaluation are deemed representative of the proposed project site.

2.5.2. *Regional Overview*

2.5.2.1. ***Temperature***

The annual average temperature for the region is 47° F. Figure 2.5-2 shows monthly average temperatures for the GCC mine site, the Casper AP site and the Douglas AP site. As illustrated, the three sites exhibit very little difference in range of temperature. Douglas AP tends to be 2º to 4° warmer during the spring and summer months, and nearly identical during the fall period. Casper is slightly cooler during December and January. July shows the highest average monthly temperatures in the region, followed by August. December and January record the lowest average temperatures for the year. Table 2.5-2 compares the monthly average temperatures for the sites.

Daily maximum temperatures in the proposed project region average approximately 59° F and daily minimum temperatures average approximately 34° F. July has the highest maximum temperatures with averages near 90° F while the lowest minimum temperatures are observed in January with averages near 10° F. Annual average minimum and maximum temperature estimates are mapped in Figures 2.5-3 and 2.5-4, respectively.

Large diurnal temperature variations are found in the region due in large part to its high altitude and low humidity. Figure 2.5-5 depicts the seasonal diurnal temperature variations for the GCC and Douglas AP sites. The site-specific monthly values are shown in Figure 2.5-2 and in Table 2.5-2. Spring and summer daily variations of 15° to 25° F are common with maximum temperature variations of 30 to 40° F observed during extremely dry periods. Less daily variation is observed during the cooler portions of the year as fall and winter have average variations of 10° to 15° F.

This reduced variation in daily temperature can be attributed to the more stable atmospheric conditions in the region during the fall and winter months. Stable periods have much lower mixing heights and accompanying lapse rates allowing for less temperature variation. The graphs in Figure 2.5-5 also show larger diurnal variations at Douglas AP than at GCC. This

may be attributed to the proximity of the site to the airport and the city of Douglas, which may provide an urban heat source which accentuates the daily maximum temperatures. It may also be influenced by the lower elevation at Douglas, which often contributes to cooler nights.

2.5.2.2. Relative Humidity

The Casper and Douglas airports record relative humidity (dew point) data. Figure 2.5-6 presents monthly relative humidity (RH) statistics for both sites. For Douglas, daily high RH peaks at 90% in May while daily low RH reaches a minimum of 21% in August. For Casper, daily high RH peaks at 78% in May while daily low RH reaches a minimum of 18% in August. The Douglas site is much closer to the North Platte River than the Casper site, perhaps accounting for the higher average relative humidity. Both seasonal and diurnal variations in RH are largely an artifact of ambient temperatures. Relative humidity is a temperature based calculation which shows the fraction of moisture present divided by the amount of moisture for saturated air at that temperature. The dew point is the temperature at which the existing moisture in the air would reach saturation, and below which moisture would begin to condense. Warm air will hold more moisture than cool air; thus, for a given mass of moisture in the atmosphere, RH will increase as the air cools.

The graph in Figure 2.5-7 presents data for Casper taken from the Wyoming Climate Atlas (WRDS, 2007). The graph shows the mean hourly relative humidity (percent) by time of day and month. The graph reflects the dry air in July and August. It also shows the winter months of December and January generally make up the most humid part of the year. The extreme values are stenciled on the graph where 25 percent is the lowest mean hourly value and 69 percent is the highest mean hourly value.

Relative humidity maximum values occur more frequently in early morning (5:00am) while minimum values typically occur during the afternoon (4:00pm). Figure 2.5-7 shows a much greater variation in the afternoon values, which coincides with the greater temperature variations.

2.5.2.3. Precipitation

The region is characterized by extremely dry conditions. On average, the region experiences only about 40 to 60 days with measurable (>0.01 in) precipitation (WRCC, 2007). The region of the proposed Ludeman Project has an annual average ranging from 11 to 12.5 inches based on interpolating regional values (Figure 2.5-8). Annual averages

across the region range from 9 to 13 inches. Spring and early summer (May-July) thunderstorms produce 45 percent of the precipitation. As shown on Figure 2.5-9, which presents average monthly precipitation data from various stations in the region, May is typically the wettest month of the year; all stations average greater than two inches for that month. January, in contrast, is the driest month of the year with precipitation averaging generally one half inch or less. The winter months (Dec-Feb) typically account for only 10 percent of the yearly precipitation totals. A secondary minimum is also evident during August, when atmospheric conditions are more stable and the absence of convective activity limits thunderstorm development.

Severe weather can occur throughout the region, but is limited on average to four or five severe events per year. These severe weather events are generally associated with hail and damaging wind events. Tornadoes can occur, but have a frequency of less than one tornado per county per year (Martner, 1986).

Major snowstorms (more than five inches/day) are relatively infrequent in the region. The region experiences less than three major snowstorms per year. Casper Airport has the highest annual snowfall of all the sites with an average of nearly 80 inches. This value is in sharp contrast to three other sites having annual averages of 20 to 25 inches (Figure 2.5-10). The discrepancy between the sites can be attributed to Casper's proximity to Casper Mountain, at the northern extreme of the Laramie Range. Casper Airport is located at the base of the northern slopes of Casper Mountain and snow events are intensified as a result of orographic lifting.

The interpolated values in Figure 2.5-11 show average snowfall of 25 to 40 inches per year in the project vicinity. This value is inconsistent with the Wyoming Climate Atlas (Martner, 1986), which lists snowfall averages for central Converse County at 50 to 60 inches. This difference results from extremely low snowfall values recorded at the Glenrock 5 ESE site, approximately 10 miles from the Ludeman site. Substantial monthly averages (more than three inches/month) occur at Glenrock 5 ESE during five months of the year and "measurable" averages (greater than one inch/month) occur seven months of the year. Based on these limited data, the timing of snowfall events in the proposed project vicinity can be predicted more reliably than the snowfall amounts.

2.5.2.4. Wind Patterns

The Douglas AP site averaged wind speeds of 10.5 mph for the 12 years included in its hourly wind database. The Casper AP site averaged wind speeds of 11.1 mph for the 18

years included in its hourly wind database. Table 2.5-3 shows the average and peak wind speeds by wind direction. The highest average wind speeds come from the west at Douglas and the south-southwest at Casper. The wind roses in Figure 2.5-13 demonstrate markedly different wind patterns at the two sites. This is due primarily to the influence of the Laramie Range to the south of Casper and southwest of Douglas.

Figure 2.5-12 graphs monthly average and maximum hourly average wind speeds for Casper and Douglas. High wind events are fairly common at both sites. Wind gusts exceed 44 mph every month of the year at Douglas, and gusts exceed 40 mph every month at Casper. Average wind speeds are highest in the spring at Dougas and in the winter at Casper. Figure 2.5-13 shows dominant winds from the west to northwest at Dougas, and the southwest at Casper. Douglas experiences a secondary mode from the southeast, primarily during the summer, while Casper is shielded by the mountains from these southeasterly winds. Data from these two sites, separated by only 50 miles, suggest that topographic features dominate wind patterns in the region.

2.5.2.5. Cooling, Heating, and Growing Degree Days

Figure 2.5-14 summarizes the monthly cooling, heating, and growing degree days for Casper, Wyoming. The data are assumed to be indicative of the region since temperatures for the various sites within the region track closely to the Casper data.

The heating and cooling degree days are included to show deviation of the average daily temperature from a predefined base temperature. In this case, 55° F has been selected as the base temperature. The number of heating degree days is computed by taking the average of the high and low temperature occurring that day and subtracting it from the base temperature. The calculation for growing and cooling degree days is the same, except that the base temperature is subtracted from the average of the high and low temperature for the day. Negative values are disregarded for both calculations.

As expected, the graphs of heating degree days and cooling degree days are inversely related and the number of growing and cooling degree days per month is identical when the same base temperature is chosen. The maximum number of heating degree days occurs in January, at 980 degree days. This coincides with January having the lowest minimum average temperature at Casper. Conversely, July registers the most cooling/growing degree days with 492, which also corresponds to July having the highest maximum average temperature.

2.5.3. *Site Specific Analysis*

The site specific discussion concentrates on meteorological data from the Ludeman Project site, with nearby data referenced for select parameters. Hourly data were collected at the Ludeman site for more than a year; The period from 2/1/2014 through 1/31/2015 is designated as the baseline year.

The project area is characterized by high plains, rolling hills and minor ridges. The vegetation types are mainly confined to native grasses with some sage brush and very sparse woody plants.

*2.5.3.1. **Monitoring Station***

The proposed project is located in Converse County approximately 15 miles northwest of Douglas, Wyoming. The project area contains nearly 30 square miles, with elevations ranging from 4,900 to 5,400 feet. It is characterized by mildly rolling terrain with a few small drainages trending southward toward the North Platte River. The meteorological monitoring station is located in the northwest corner of the project permit boundary. It is situated in an open area deemed most representative of meteorological conditions affecting the proposed satellite processing plant and surrounding well fields.

Hourly values are recorded at the Ludeman met station for:

- Average horizontal wind speed at 10 meters;
- Peak horizontal wind speed (5-second wind gust) at 10 meters;
- Average horizontal wind direction at 10 meters;
- Average standard deviation of horizontal wind direction;
- Average ambient temperature at 2 meters;
- Average ambient temperature at 10 meters;
- Average difference in ambient temperature between 2 meters and 10 meters (calculated temperature lapse rate or delta-T);
- Average relative humidity;
- Sample barometric pressure;
- Total precipitation; and
- Average solar radiation.

Table 2.5-4 lists the instruments employed at the Ludeman met station and the related specifications.

Table 2.5-5 summarizes meteorological conditions at the Ludeman site. It also shows data recovery for the baseline year, which exceeded 99% for all monitored parameters.

2.5.3.2. Temperature

Figure 2.5-15 shows monthly average temperatures ranging from 19° F in February to 71°F in July. Daily high temperatures averaged 32° F in February and 84° F in July. Daily low temperatures averaged 14° F in February and 58° F in July. During the baseline monitoring period temperature extremes ranged from -19° F in February to °93 F in July. The average project site temperature during this 12-month period was 45.5º F.

GCC is approximately 15 miles northwest of the Ludeman site, Casper is 40 miles to the west, and Douglas is approximately 15 miles to the southeast. Figure 2.5-16 illustrates similar monthly temperature profiles between Ludeman and these neighboring meteorological stations. The apparent anomaly in February is a consequence of an unusually cold February in 2014. Casper, Douglas and GCC averages represent long-term periods, whereas Ludeman averages reflect only the baseline monitoring year. The average temperature at Douglas during Feburary of 2014 was 18.4° F, and the Casper average was 19.5° F. Both these values are consistent with Ludeman.

Figure 2.5-17 shows an average diurnal temperature swing at the Ludeman site of 27° F in summer and 10° F in the winter.

2.5.3.3. Wind Patterns

Figure 2.5-18 shows the annual and seasonal wind roses for the Ludeman site. The predominant wind direction is westerly, with high winds also coming from the west-southwest and a secondary east-southeast mode. These two modes are heavily influenced by the east-west trending mountain range to the south. High pressure located over the southwestern United States produces the strong west/southwesterly winds characteristic of central and western Wyoming. Spring exhibits the greatest variability in wind direction with secondary modes from the east-southeast and northerly directions. These secondary modes are a result of the synoptic scale transition period that occurs during spring. Low pressure regions develop on the lee side of the Rockies bringing southeasterly and east-

southeasterly winds during development. As the low pressure systems form and move off with the general atmospheric flow, winds switch to a northerly direction.

Figures 2.5-19 and 2.5-20 compare the Ludeman site wind rose to the GCC and Douglas wind roses. These comparisons emphasize the pronounced influence of local topography. GCC winds show a stronger west-southwesterly component typical of the region to the northwest of the Laramie Range. Douglas winds show stronger northwesterly and southeasterly components typical of the eastern slopes of Wyoming's north-south trending mountain ranges. These differences may be attributed in part to the funneling of northwesterly winds and the shielding of southeasterly winds by the Laramie Range at the Ludeman site. The same mountains shield Douglas from the west-southwesterly winds prominent at Ludeman, but do not block or redirect winds emanating from the north to northwesterly directions. The Glenrock location exhibits greater similarity to the Ludeman site than Douglas, perhaps owing to its similar relationship to the mountains. Glenrock is slightly farther from the mountain range and higher than the Ludeman site

The monthly wind speeds at Ludeman are summarized in Figure 2.5-21. Monthly maximum and average wind speeds both occur in early spring and late fall, with the lowest wind speeds evident during the summer months. Figure 2.5-22 shows the diurnal variation in wind speed by calendar quarter. The lowest wind speeds occur during summer months and the highest wind speeds occur during winter months. The strongest winds typically occur during afternoon hours, regardless of season. Figure 2.5-23 shows the wind speed frequency and cumulative frequency distributions. The median wind speed is 11 mph and winds average over 18 mph 20% of the time.

Table 2.5-6 contains the Joint Frequency Distribution for the Ludeman site. The distribution shows the frequencies of hourly average wind speed for each direction based on stability class. Seventy percent of all winds at Ludeman fall into stability class D which represents near neutral to slightly unstable conditions. The light winds which accompany stable environments can be seen by the Stability Class F summary, which shows the lowest total frequency of all the stability classes.

2.5.3.4. Precipitation

Monthly precipitation totals are shown in Figure 2.5-9. June was the wettest month, with December recording only 0.01 inches of precipitation. Total precipitation for the baseline year was 7.94 inches. Figure 2.5-24 plots monthly precipitation totals during the baseline year. Most of the precipitation fell during the summer months.

2.5.3.5. Relative Humidity

Figure 2.5-25 graphs monthly average relative humidity (RH), as well as average daily high and low RH by month. Average RH values range from 50% in July to nearly 75% in February. Daily high, hourly average RH peaks at 90% in May while daily lows reach a minimum of 30% in July. Figure 2.5-26 shows the diurnal variation. Diurnal swings in RH are more pronounced during the warmer months, paralleling seasonal and diurnal variations in ambient temperatures.

2.5.3.6. Solar Radiation

Figure 2.5-27 graphs average solar radiation by month. Solar radiation values are used, along with wind speeds, daily high/low temperatures and daily high/low relative humidity to estimate monthy evapotranspiration (ET) using the Penman Equation. ET serves as an estimate of pan evaporation. Figure 2.5-28 summarizes the ET calculation results, which lead to an annual ET of 60 inches. Typical pan evaporation rates in central Wyoming range from 45 to 59 inches per year (Martner 1986).

2.5.3.7. Atmospheric Stability

Figure 2.5-29 compares the atmospheric stability class distribution at Ludeman based on two different calculation methods. By the sigma-theta (σ_θ) method, atmospheric stability classes were assigned to each hour as described in EPA guidance (EPA 2000). Alternatively, these classes were also derived from solar radiation and temperature gradient (SRDT method). Figure 2.5-29 shows that stabiity Class D, designated as neutral to slightly unstable conditions, dominates for both methods.

2.5.3.8. Upper Atmosphere Characteristics

The nearest upper-air data available from the National Weather Service is from Riverton, Wyoming or Rapid City, South Dakota. In both cases, the large distance from the southern PRB and the proximity to prominent mountain ranges make them ill suited to represent the proposed project site.

The Air Quality Division of the Wyoming Department of Environmental Quality (WDEQ-AQD) has provided statewide mixing heights to be used in dispersion modeling with the

Industrial Source Complex (ISC3) model. For modeling purposes, the annual average mixing heights are assigned according to stability class as follows:

Class A	3,450 meters
Class B	2,300 meters
Class C	2,300 meters
Class D	2,300 meters
Class E	10,000 meters
Class F	10,000 meters

Stability classes E and F are given an arbitrarily high number to indicate the absence of a distinct boundary in the upper atmosphere. Based on the exclusive use of these numbers for air quality modeling by mines in the Powder River Basin, dispersion modeling with ISC3 has used the mixing heights provided by the WDEQ/AQD.

In August of 2000, IML Air Science conducted Sound Detection and Ranging (SODAR) monitoring at the Black Thunder Mine, located approximately 40 miles north-northeast of the proposed Ludeman Project site. The purpose of this monitoring was to support a comprehensive study of NO_x dispersion characteristics following overburden removal and coal blasting events. The SODAR instrument provided 3D wind speeds, wind directions, temperatures, temperature gradients, and other atmospheric parameters as a function of height above the ground. The vertical range of the SODAR was 1,500 meters, with a sounding performed every 15 minutes. Each sounding resulted in a calculated "inversion height / mixing height" (the two terms are used interchangeably by the SODAR system supplier). These mixing heights were downloaded into a database and queried, with results shown in Table 2.5-7. Morning and afternoon time intervals were taken from EPA modeling guidance.

The SODAR definition of mixing height appears somewhat ambiguous, and these measurements were all taken in August. Therefore, they are presented here as an additional data source, but not recommended as direct meteorological inputs to the MILDOS model. The default mixing height for MILDOS is conservative, at 100 meters.

2.5.3.9. Bodies of Water and Special Terrain Features

The North Platte River is the only significant body of water in the vicinity of the proposed project site. Most of the proposed Ludeman project activities would occur in the hills north of the river, minimizing the river's influence on the proposed project site's meteorology.

Terrain features that influence the general meteorological conditions at the proposed Ludeman site include the Laramie Range to the south, the North Platte valley, and nearby drainages that support small, ephemeral streams. The maximum topographic relief within the project area is a few hundred feet.

2.5.3.10. Air Quality

National Ambient Air Quality Standards (NAAQS) exist for sulfur dioxide (SO_2), nitrogen dioxide (NO_2), carbon monoxide (CO), ozone (O_3), lead, and particulate matter small enough to move easily into the lower respiratory tract. EPA tracks particles less than ten micrometers (μm) in aerodynamic diameter, designated PM_{10}, and particles less than ten μm, designated $PM_{2.5}$. The NAAQS are expressed, as pollutant concentrations that are not to be exceeded in the ambient air, that is, in the outdoor air to which the general public has access (40 CFR Part 50.1(e)). Primary NAAQS are designated to protect human health; secondary NAAQS are designated to protect human welfare by safeguarding environmental resources (such as soils, water, plants, and animals) and manufactured materials. Primary and secondary NAAQS are presented in Table 2.5-9.

The air quality in the proposed project region is considered to be very good. The area is sparsely populated and is not heavily developed with major sources of industrial air pollution. The closest air quality monitoring station to the proposed project area is in Douglas, Wyoming at an approximate distance of 15 miles from the project area. This station shows that regional air quality is well within compliance with the NAAQS, which for particulate matter are equivalent to the Wyoming Ambient Air Quality Standards (WAAQS). Table 2.5-8 summarizes recent PM_{10} and $PM_{2.5}$ monitoring results from Douglas and compares them to the WAAQS (EPA 2015).

In addition to ambient air quality standards, which represents an upper bound on allowable pollutant concentrations, there are also national standards for the Prevention of Significant Deterioration (PSD) of air quality (40 CFR § 51.166). The PSD standards differ from the NAAQS in that the NAAQS provide maximum allowable concentrations of pollutants, while PSD requirements provide maximum allowable increases in concentrations of pollutants for areas already in compliance with the NAAQS. PSD standards are therefore expressed as allowable increments in the atmospheric concentrations of specific pollutants. Allowable PSD increments currently exist for three pollutants: NO_2, SO_2, and PM 10. Increments that is particularly relevant when a major proposed action (involving either a new source or a major modification to an existing source) may degrade air quality without exceeding the NAAQS, as would be the case in an area where the ambient air is considered

to be very clean. One set of allowable increments exists for Class II areas, which cover most of the continental United States. A much more stringent set of allowable increments exists for Class I areas, which are special designated areas where the degradation of ambient air quality is severely restricted. Class I areas include certain national parks and monuments, wilderness areas, and other areas as described in 40 CFR § 51.166(e) and 40 CFR Part 81:400-437. Maximum allowable PSD increments for Class I and Class II areas are given in Table 2.5-10. A Class I area that is in proximity to the proposed Ludeman facilities is the Thunder Basin National Grasslands. PSD Class I areas receive the highest degree of protection from air pollution. Only small amounts of particulate, consisting of SO_2, and NO_2 air pollutants, are allowed in Class I areas (BLM, 2004c).

The primary new emission source of non-radiological pollutants will be particulate matter with a diameter less than ten micrometers (PM_{10}) resulting from vehicle traffic within the proposed Ludeman Project Area. Projected activities impacting fugitive dust emissions included ongoing wellfield construction activities, routine site traffic related to operations and maintenance, heavy truck traffic delivering chemicals and material and product shipping, and employee traffic to and from the site. Based on these activities, the projected total PM_{10} emissions is 15.5 tons per year. This level of emissions is considered quite small relative to surface mines and other industrial operations that generate dust from vehicles and disturbed areas. The larger surface mines in the Powder River Basin show PM_{10} emissions inventories in the thousands of tons per year. Sections of unpaved county roads can also exceed 15.5 tons per year emission rate by an order of magnitude or more. Atmospheric dispersion modeling typically shows that fugitive PM_{10} emissions on the order of 100 tons per year results in insignificant impacts to ambient air quality beyond a distance of a few hundred meters from the sources. Significant impact for PM_{10} is defined as 1.0 μg/m3 or more. The WAAQS for annual average PM_{10} is 50 μg/m3. Since the estimated 100 tons per year of PM_{10} fugitive dust emissions is well below the 250 tons per year threshold for PSD review, an analysis to further determine possible impacts to ambient air quality are considered unnecessary.

2.5.4. *Demonstration of Long-Term Representativeness of On-Site Data*

In response to previous guidance from NRC, the following section applies alternative statistical tests to the comparison of short and long-term, hourly wind speed and wind direction data at a representative site (Casper Airport). The alternatives considered include summary statistics, the chi-square test, the Student's t-test, the Kolmogorov-Smirnov test, and linear correlation/regression analysis. A separate report documents and evaluates these alternative tests for their appropriateness in comparing meteorological frequency

distributions (IML 2014). The report presents a case study based on three sites with available long-term meteorological data. This allows temporal comparisons for each site, as well as inter-site comparisons to assess how well each statistical test discriminates between visually similar and dissimilar frequency distributions.

2.5.4.1. Data Sources

Uranium One Americas has collected over one year of hourly meteorological data at its Ludeman ISR Project site (IML 2015). For the purposes of MILDOS modeling and this analysis, the first year serves as the baseline period. For comparing long-term meteorological conditions to short-term conditions, hourly data from the Casper Airport (NCDC 2015) were used. Casper was selected due to several factors:

1. Operated by the National Weather Service, meeting NRC guidance in Regulatory Guide 3.63;
2. Proximity to the Ludeman Project site (40 miles to the west), similar elevation, terrain and relationship to east-west trending mountain range to the south; and
3. Longest period of record within a 50-mile radius, with 18 years of hourly data available in electronic form.

The short-term period is synchronous with the baseline monitoring year at the Ludeman site, from February 1, 2014 through January 31, 2015. The long-term period is defined as 1997 through 2013, or 17 calendar years. Thus, there is no overlap between short-term and long-term data sets. Hourly wind speed and wind direction data are categorized to form short and long-term frequency distributions. Wind speeds are divided into 6 classes (plus a 7^{th} calm class), and wind directions are divided into 16 classes (plus a 17^{th} calm class). These classification schemes correspond directly to the MILDOS STAR distribution. Appropriate statistical tests from the list enumerated above, are employed to determine if there is a significant difference between the short and long-term distributions of classified Casper data.

Notwithstanding the example of 30 years cited in NRC Regulatory Guide 3.63, 17 years are deemed adequate to represent long-term meteorological data. A separate report documents this (IML 2014) and cites the risks of using too long a period of record (POR). In particular, a publication from the U.S. Air Force Climatology Center (Coffin 1996) states, "As the POR expands, maintaining homogeneity of the data becomes more difficult. Climatological statistics obtained from too long a period may not be representative of contemporary conditions."

2.5.4.2. Graphical Methods

Graphical methods can be useful in comparing meteorological data sets (Gardiner 1979). Histograms, scatterplots and wind roses provide a visual demonstration of the similarities between short and long-term meteorological data at Casper. Figure 2.5-30 compares the 1-year (baseline) and 17-year wind frequency distributions. It can be seen that both wind speed and wind direction frequencies are distributed similarly over the two time periods.

Figure 2.5-31 shows the wind roses from Casper for the same periods, with very little apparent differences. The wind rose provides a polar graph of the joint distribution of wind speed and wind direction frequencies.

Figure 2.5-32 graphs the short-term vs. long-term wind frequencies, demonstrating close correlation between the two wind speed distributions and between the two wind direction distributions. In this instance, the right-most point on the wind speed graph corresponds to the 8-12 mph category, which accounts for 27% of the hourly wind speeds for the baseline year (y-axis), and 28% of the hourly wind speeds over the previous 17 years (x-axis). The other points correspond to the remaining 6 wind speed categories. The wind direction graph plots the 17 direction categories in similar fashion.

Figure 2.5-33 graphs the short-term vs. long-term joint wind speed and direction frequencies, once again demonstrating close correlation between the two periods for each of the 97 joint categories. Figure 2.5-33 substantiates the similarity between wind roses in Figure 2.5-31.

2.5.4.3. Summary Statistics

Table 2.5-11 shows the average wind speed, unit-vector averaged wind direction, and vector averaged wind direction for the 17-year monitoring period and for the 1-year baseline period. Between the two periods, these statistics are quite similar.

2.5.4.4. Application of the Chi-Square (χ^2) Test

The χ^2 test can be used to evaluate the null hypothesis (H_0) that two frequency distributions are similar. A separate report (IML 2014) demonstrates some limitations in the χ^2 test when applied to frequency distributions derived from large samples. It discusses the

usefulness of converting relative frequencies to equivalent annual hours, then adjusting the χ^2 value for large sample size by means of the phi coefficient.

In this analysis, the χ^2 test regards long-term values as the expected hourly counts per year, and short-term (baseline period) values as the observed counts per year. Table 2.5-12 shows the resulting analysis of wind speeds at Casper. The calculated χ^2 value of 39.70 is more than the 95% confidence statistic for 6 degrees of freedom (12.59). Thus, for this sample size (8,760) we reject H_0, which states that the short-term wind speed distribution comes from the same population as (i.e., is representative of) the long-term distribution. However, due to the liabilities of the Chi-Square test in treating large samples (IML 2014), we compute the phi coefficient, which adjusts the χ^2 result for large sample sizes, as 0.07. This infers similarity between the two wind speed distributions. An analysis of categorized cloud cover by the U.S. Air Force established a critical phi coefficient of 0.20, below which "a large degree of similarity" between distributions is indicated (Lowther 1991). Note that the minimum annual count of 455 (0 - 3 mph) is larger than the minimum recommended by NRC (NRC 2011) for a valid χ^2 test.

Table 2.5-13 shows a similar test for 17-year vs. 1-year wind directions at Casper. The calculated χ^2 value of 48.96 is more than the 95% confidence statistic for 16 degrees of freedom (26.30), so we initially reject the null hypothesis (H_0) that the short-term wind direction distribution comes from the same population as the long-term distribution. The phi coefficient of 0.07, however, suggests a strong similarity between the two wind direction distributions. As with wind speeds, the minimum annual count of 68 (SSE) is sufficient for a valid χ^2 test.

If the wind direction frequencies are multiplied by 1,000 rather than by 8,760, the χ^2 test in Table 2.5-13 produces a different outcome (Table 2.5-14). In this case the calculated χ^2 value of 5.59 is less than the critical value, so we cannot reject H_0 with 95% confidence. As pointed out above, the χ^2 test is sensitive to large sample sizes. The phi coefficient removes this sensitivity. Though the χ^2 statistics are different, a sample size of 1,000 (Table 2.5-14) and a sample size of 8,760 (Table 2.5-13) both yield the same phi coefficient of 0.07. Neither version of the test ultimately provides sufficient evidence to reject H_0.

Table 2.5-15 shows the χ^2 test for wind speed frequencies multiplied by 1,000 instead of 8,760. The χ^2 statistic of 4.53 indicates non-rejection of H_0. The phi coefficient of 0.07 confirms this and is independent of the choice of sample size, again offering a more reliable measure of similarity.

These χ^2 test results indicate insufficient evidence to infer a statistical difference between short and long-term wind speed and wind direction distributions. This is not always the case. A separate report (IML 2014) illustrates that even when corrected for large samples, the χ^2 test generally infers a significant difference between wind frequency distributions from different sites.

2.5.4.5. Evaluation of the Student's T-Test

The two-sample t-test can be used to assess similarity between two frequency distributions, if those distributions are expanded to form year-to-year frequencies within each individual data category. Two-sample t-tests conducted in the manner of the χ^2 test discussed above were eliminated. Such a test evaluates differences between two complete frequency distributions, but in this application the short and long-term frequencies will always have the same mean (1/C, where each of the paired distributions has C categories). Under these circumstances the t-test will always show equivalence (IML 2014).

Alternatively, the two-sample t-test can be applied separately to each wind speed and wind direction category. This scenario is only effective when comparing two multi-year distributions, since both short-term and long-term variability are needed. Therefore, this approach is not practical for the single-year baseline monitoring period at the Ludeman site.

2.5.4.6. Evaluation of the Kolmogorov-Smirnov Test

The Kolmogorov-Smirnov (K-S) test is a nonparametric test for the equality of continuous, one-dimensional probability distributions that can be used to compare two samples without many of the assumptions required for other statistical methods. In exchange for this broad applicability, the K-S test sacrifices statistical efficiency. A case study shows that all inter-site comparisons using the K-S test result in the false conclusion that the wind speed and wind direction distributions are statistically no different (IML 2014). The respective wind roses, the χ^2 test, and linear regression analysis all contradict this result. While its consistent finding of insignificant differences superficially supports the case for representativeness, the inability of the K-S test to distinguish between clearly dissimilar wind patterns eliminates this method as an appropriate alternative.

2.5.4.7. Application of Linear Correlation and Linear Regression

The following discussion combines linear correlation and regression since they yield closely related statistics. Linear regression is used to compare wind speed and wind direction frequency distributions for several reasons:

1. To make the correlation visible (shows line of least-squares fit).
2. To isolate the percentage of inter-category variance that is predictable (R^2) from the percentage that is random ($1 - R^2$), an important measure of how well one frequency distribution represents another.
3. To enable a zero intercept, providing a slightly more conservative R^2. A non-zero intercept implies a systematic bias, which is technically not possible between two frequency distributions that each sum to one.

Linear regression, without a forced zero intercept, produces a coefficient of determination R^2 which is precisely the square of the Pearson coefficient R generated by linear correlation. With the forced zero intercept this relationship is only approximate, but always errs on the side of conservatism (i.e., the square root of the coefficient of determination is always less than or equal to the correlation coefficient). While linear regression has not been commonly employed to demonstrate the degree of similarity between two meteorological frequency distributions, linear correlation coefficients have (Coffin 1996). A separate report (IML 2014) offers an in-depth analysis of linear correlation and regression in the context of meteorological frequency distributions.

A correlation coefficient is merely a mathematical expression of the "correspondence" between two distributions (Brooks 1978). In the present application, the short and long-term data distributions both approximate a third variable, the true long-term distribution. If any two relative frequency distributions of a categorized meteorological parameter are linearly correlated, they are also substantially equivalent since the frequencies sum to 1 for both distributions. And if they are equivalent, then either they both represent the true long term distribution, or neither does.

Figure 2.5-34 illustrates the linear association between short and long-term wind speed frequencies at Casper. In keeping with convention, the less certain variable (short-term frequency) is assigned to the vertical (dependent) axis and the better-supported, long-term frequency is assigned to the horizontal (independent) axis. The hourly data for each distribution fall into one of 7 categories. The graph illustrates the degree to which the 1-year frequencies match the 17-year frequencies. The R^2 value of 0.983 confirms a very strong linear relationship, and the slope of 0.992 indicates substantial equivalence between

short and long-term frequencies. A p-value of zero establishes a near-100% confidence level that this relationship is significant.

Figure 2.5-35 illustrates the linear association between short and long-term wind direction frequencies at Casper, with the same choice of dependent and independent variables. The hourly data for each distribution fall into one of 17 categories. The graph illustrates the degree to which the 1-year frequencies match the 17-year frequencies. The R^2 value of 0.991 confirms a strong linear relationship, and the slope of 0.988 indicates substantial equivalence between short and long-term frequencies. A p-value of zero leaves little doubt that this relationship is significant.

The MILDOS model accepts meteorological inputs in the form of joint wind speed, wind direction and stability class frequency distributions, also known as STAR distributions. An important subset of the STAR distribution is the two-way wind classification, which categorizes hourly wind data by both speed and direction. Hypothesis testing is generally unworkable in comparing joint wind speed and direction frequencies because the wind data are partitioned into too many categories. In general, the number of categories in hypothesis testing should not exceed $5*\log_{10}(N)$, where N is the sample size (Brooks 1978). For a one-year sample of hourly averages (N = 8,760) the maximum number of categories would be 20. This limit is consistent with 7 wind speed classes or 17 wind directions, but not with 97 joint frequency categories. Therefore the χ^2 test is not appropriate for evaluating similarities between joint frequency distributions.

Joint wind speed and direction distributions are amenable to linear regression or correlation. Analyzing these two-way distributions can strengthen the case for long-term representativeness of baseline wind data. The joint analysis offers a more rigorous comparison between short and long-term wind frequency distributions, than individual speed and direction analyses. This comparison also offers the best quantitative measure of the similarity between the associated wind roses.

Figure 2.5-36 shows the linear relationship between short and long-term joint frequencies at Casper. The hourly data for each distribution fall into one of 97 categories. The graph illustrates the degree to which the 1-year joint frequencies match the 17-year frequencies. The R^2 value of 0.979 confirms a very strong linear relationship, and the slope of 0.988 indicates substantial equivalence between short and long-term frequencies. A p-value of zero leaves little doubt that this relationship is significant.

Figure 2.5-37 graphs a short-term joint frequency distribution against the longer-term joint frequency distribution from the Douglas Airport, with similar results. Douglas also exhibits

strong temporal correlation of joint wind frequencies. Figure 2.5-38 graphs the long-term joint frequency distribution from Douglas against that from Casper. The R^2 value of 0.108 indicates virtually no similarity between the two sites. The contrast to Figures 2.5-36 and 2.5-37 illustrates how effectively linear regression discriminates between similar and dissimilar wind regimes.

Linear regression also isolates the sources of variation among category frequencies. When multiplied by 100, R^2 signifies the percent of the variation from a mean frequency that is common to both short and long-term distributions. In Figure 2.5-36, for example, 99% of the variation among 1-year joint frequencies can be predicted based on measured long-term frequencies, while only 1% is attributed to random, year-to-year fluctuations and/or measurement error. In Figure 2.5-38, only 11% of the variation at Douglas can be explained by the observed wind patterns at Casper.

Linear correlation produces Pearson's correlation coefficient R, based on the assumption of normally distributed data. The normality assumption can be relaxed by ranking the data and computing Spearman's correlation coefficient, a method commonly applied to nonparametric data. The Casper wind speed comparison yields a Pearson's R of 0.992 and a Spearman's R of 0.964. The Casper wind direction comparison yields a Pearson's R of 0.996 and a Spearman's R of 0.990. Therefore, the assumption of normally distributed data does not compromise the results. A separate report shows that the Spearman's and Pearson's coefficients are typically similar for wind frequency distributions (IML 2014).

2.5.4.8. Conclusion

In fulfillment of NRC guidelines, the combination of visual evidence, summary statistics, linear correlation and hypothesis testing provides a comprehensive demonstration of long-term representativeness of baseline meteorological data at the Ludeman ISR Project site. For the Casper Airport site, the baseline year of hourly wind data are statistically no different than the previous 17 years of data. This conclusion is supported by graphical analyses and by two statistical tests, which have been jointly applied by others to categorize meteorological data (Lowther 1991):

1. χ^2 test (with the phi coefficient to adjust for large sample size); and
2. Linear correlation coefficient R (or coefficient of determination R^2).

Table 2.5-16 summarizes the test results from Casper wind data. For wind speed, wind direction, and joint frequency distributions, all relevant statistical tests infer the absence of a significant difference between short and long term data.

The χ^2 test gives a yes/no answer: either the computed statistic results in 95 percent confidence in a significant difference, or it does not. Linear regression supplies the best measure of the degree of similarity between short-term and long-term wind speed, wind direction and joint frequency distributions. It is uniquely suited to testing joint wind speed and direction frequencies due to the large number of categories.

Casper is considered to be representative of the Ludeman site due to its proximity, similar elevation, comparable terrain, relationship to the east-west trending mountain range to the south, and susceptibility to the same regional climatological factors. With the above demonstration of baseline-year representativeness of long-term wind conditions at Casper, it is reasonable to conclude that baseline-year monitoring at Ludeman also represents the long-term.

2.5.5. *References*

Brooks 1978, *Handbook of Statistical Methods in Meteorology*, C. E. P. Brooks and N. Carruthers, Reprint of 1953 Edition, 1978.

Coffin 1996, *Consolidated Statistical Background Papers*, U.S. Air Force Climatology Center, Charles R. Coffin, November 1996Curtis, J. and K. Grimes, 2007: *Wyoming Climate Atlas.* Available: http://www.wrds.uwyo.edu/wrds/wsc/climateatlas/ [2007,May 2].

EPA 2015, *AirData Access to Monitored Air Quality Data from EPA's Air Quality System (AQS) Data Mart*, Accessed December 2015, http://www3.epa.gov/airdata/index.html

EPA 2000, *Meteorological Monitoring Guidance for Regulatory Modeling Applications*, EPA-454/R-99-005, February 2000

Gardiner 1979, *Analysis of Frequency Distributions, Concepts and Techniques in Modern Geography*, V. Gardiner & G. Gardiner, 1979.

IML 2015, *Meteorological Monitoring Database for Ludeman ISR Project*, IML Air Science, Period of Record January, 2014 through February, 2015.

IML 2014, *Evaluation of Alternative Methods to Demonstrate Long-Term Representativeness of Baseline-Period Meteorological Monitoring at In-Situ Uranium Projects*, IML Air Science, June 2014.

Lowther 1991, *RTNEPH Total Cloud Cover Validation Study*, Capt Ronald P. Lowther, Mr. Mark T. Surmeier, Capt Richard W. Hartman, Mr Charles R. Coffin, Capt Anthony J. Warren, November 1991.

Martner 1986, *Wyoming Climate Atlas*. Martner, B.E., University of Nebraska Press, Lincoln, NE.

NCDC 2015, *Quality Controlled Local Climatological Data,* National Climatic Data Center accessed 2/19/2015. http://cdo.ncdc.noaa.gov/qclcd/QCLCD?prior=N

NCDC 2007, *Surface Data, Monthly Extremes.* National Climatic Data Center Available: http://gis.ncdc.noaa.gov/website/ims-cdo/extmo/viewer.htm?Box=-

110.307738654357:41.4493000825986:-102.349767058746:45.2536595444503 [2007, July 13].

WRCC 2007, *Local Climate Data Summaries*. Western Region Climate Center Available: http://www.wrcc.dri.edu/summary/lcd.html [2006, Jan 28].

TABLES

Table 2.5-1: Meteorological Stations Included in Climate Analysis

Station Name	Agency	X (UTM)	Y (UTM)	Z (ft)	Period of Record
Antelope Coal Company	IML	474179	4816180	4675	1986-2007
Casper Airport (112)	NWS	380229	4750539	5338	1948-2014
Douglas Airport (118)	NWS	468655	4732910	4820	1909-2014
Dull Center 1 SE (71)	NWS	503239	4806131	4420	1926-2005
Glenrock 5 ESE	NWS	435609	4741868	4948	1948-2008
Glenrock Coal Company	IML	431649	4767610	5674	1996-2007
Kaycee (58)	NWS	368677	4840739	4660	1900-2005
Lance Creek 3 WNW (77)	NWS	528436	4782869	4340	1962-1984
Ludeman Project On-Site	IML	444386	4752034	5342	2014-2015
Midwest (59)	NWS	396362	4806926	4820	1939-2005
Reno (68)	NWS	458891	4836243	5080	1963-1983

Table 2.5-2: Annual and Monthly Average Temperatures in Proximity of Project

	Jan	Feb	Mar	Apr	May	Jun	Jul	Aug	Sep	Oct	Nov	Dec	Ann
Casper AP	23.4	27	33.9	42.8	52.5	62.8	71	69.2	58.5	46.5	33.4	25	45.5
Douglas AP	26.9	25.3	35.6	43.7	53.3	64.5	74.2	69.5	57.7	45.8	34.0	24.5	47.7
Glenrock	26.1	26.7	32.5	41.7	51.1	60.7	70.8	68.1	57.9	45.7	33.7	26.1	46.1

Table 2.5-3: Wind Parameters by Direction Sector (NCDC, 2015)

Wind Direction	Douglas Wind Speed (mph)	Douglas Max Wind Gust	Casper Wind Speed (mph)	Casper Max Wind Gust
N	3.8	39.1	4.9	41.0
NNE	10.4	40.3	10.8	41.0
NE	10.0	33.4	9.2	44.0
ENE	10.3	32.0	9.1	34.0
E	9.2	33.4	9.4	34.0
ESE	10.2	35.7	7.4	28.0
SE	12.3	38.0	6.6	29.0
SSE	9.9	43.7	6.8	32.0
S	7.6	29.9	9.3	43.3
SSW	9.3	31.1	16.4	51.0
SW	11.8	48.0	15.4	55.4
WSW	15.2	47.0	12.1	45.6
W	16.5	52.9	10.3	45.0
WNW	13.4	54.1	9.8	39.0
NW	11.9	45.0	8.5	36.0
NNW	11.7	48.0	8.0	38.0

Table 2.5-4: Ludeman Meteorological StationMonitoring Instruments

Parameter	Instrument	Range	Accuracy	Threshold	Instrument Height
Wind Speed	RM Young 05305 Wind Monitor AQ	0 to 112 mph	±0.4 mph or 1% of reading	0.9 mph	10 meters
Wind Direction	RM Young 05305 Wind Monitor AQ	0 to 360º	±3º	1.0 mph	10 meters
Temperature	RM Young RTD Temperature Probe Assembly	-25º to 50º C	±0.2º C @ given range	-- º C	2 meters
Temperature	RM Young RTD Temperature Probe Assembly	-25º to 50º C	±0.2º C @ given range	-- º C	10 meters
Temperature Lapse Rate	RM Young RTD Temperature Probe Assembly	Difference Calculation	±0.1º C	-- º C	2 meters
Relative Humidity	CS 215 Temp and RH Probe	0 to 100%	±2% at 23º C	--	2 meters
Barometric Pressure	Vaisala CS106 Barometer	0 to 944" Hg	0.25%	--	2 meters
Precipitation	Texas Electronics 8” Heated Tipping Bucket Precipitation Gauge	0 to 10 in/hr	±0.5% @ 0.5 in/hr rate	0.01”	1 meter
Solar Radiation	Apogee CS300 Pyranometer	0 to 2,000 w/m^2	±5%	--	2 meters
Data Logger	Campbell Scientific CR1000 Data Logger	--	--	--	--

Table 2.5-5: Ludeman Meteorological Monitoring Summary

Ludeman Project Baseline Year

Meteorological Data Summary

2/1/2014 - 1/31/2015

Hourly Data

	Average/Total	Max	Min
Wind Speed (mph)	14.1	47.8	0.4
Sigma-Theta (°)	15.3	100.6	0.2
Temperature (F)	45.5	93.3	-18.5
10m Temperature (F)	45.8	91.9	-18.0
Relative Humidity (%)	62.2	99.2	14.7
Precipitation (in)	7.34	0.63	
Bar. Pressure (in Hg)	24.6	25.2	24.0
Solar Radiation (w/m^2)	171.0	939.0	

Predominant wind direction was from the W sector,
accounting for 24.2% of the possible winds

Data Recovery

Parameter	Possible (hours)	Reported (hours)	Recovery
Wind Speed	8760	8756	99.95%
Wind Direction	8760	8756	99.95%
Sigma-Theta	8760	8756	99.95%
Temperature	8760	8756	99.95%
10m Temperature	8760	8756	99.95%
Relative Humidity	8760	8756	99.95%
Precipitation	8760	8694	99.25%
Bar. Pressure	8760	8756	99.95%
Solar Radiation	8760	8754	99.93%

Table 2.5-6: Ludeman Site Joint Frequency Distribution for Baseline Year

Ludeman ISR Project — Frequency Distribution — IML Air Science
Glenrock, Wyoming — Hourly Average Wind Speed, Wind Direction and Sigma — Sheridan, WY
Calm Readings 12 Total Readings 8756 Possible Readings 8760 Data Capture 100.0%
From 2/1/2014 To 1/31/2015

Stability Class A — **Wind Speed (mph)**

Direction	< 3	4 - 7	8 - 12	13-18	19 - 24	> 24	Row Total
E	0.00129	0.00183					0.00312
ENE	0.00035	0.00171					0.00206
ESE	0.00117	0.00217					0.00334
N	0.00047	0.00126					0.00172
NE	0.00047	0.00160					0.00207
NNE	0.00059	0.00091					0.00150
NNW	0.00035	0.00114					0.00149
NW	0.00070	0.00137					0.00207
S	0.00129	0.00308					0.00437
SE	0.00164	0.00320					0.00484
SSE	0.00164	0.00263					0.00427
SSW	0.00246	0.00240					0.00486
SW	0.00187	0.00263					0.00450
W	0.00152	0.00240					0.00392
WNW	0.00117	0.00183					0.00300
WSW	0.00187	0.00274					0.00462
Sum	0.01886	0.03289					0.05175

Table 2.5-6 (Cont.)

From 2/1/2014 To 1/31/2015

Stability Class B **Wind Speed (mph)**

Direction	< 3	4 - 7	8 - 12	13-18	19 - 24	> 24	Row Total
E	0.00012	0.00160					0.00172
ENE	0.00012	0.00160	0.00011				0.00183
ESE	0.00012	0.00377	0.00057				0.00446
N		0.00091	0.00023				0.00114
NE	0.00012	0.00069					0.00080
NNE		0.00057					0.00057
NNW		0.00103	0.00011				0.00114
NW		0.00137	0.00023				0.00160
S	0.00035	0.00080					0.00115
SE	0.00047	0.00377	0.00023				0.00447
SSE	0.00012	0.00057	0.00011				0.00080
SSW	0.00023	0.00057	0.00011				0.00092
SW	0.00012	0.00228	0.00011				0.00252
W		0.00251	0.00034				0.00286
WNW	0.00012	0.00297	0.00023				0.00331
WSW	0.00047	0.00194	0.00011				0.00252
Sum	0.00234	0.02695	0.00251				0.03181

Table 2.5-6 (Cont.)

From 2/1/2014 To 1/31/2015

Stability Class C **Wind Speed (mph)**

Direction	< 3	4 - 7	8 - 12	13-18	19 - 24	> 24	Row Total
E	0.00023	0.00137	0.00217				0.00377
ENE	0.00012	0.00080	0.00183				0.00274
ESE		0.00137	0.00674				0.00811
N		0.00034	0.00480				0.00514
NE		0.00023	0.00137				0.00160
NNE		0.00023	0.00183				0.00206
NNW		0.00011	0.00434				0.00445
NW		0.00023	0.00354				0.00377
S		0.00011	0.00034				0.00046
SE		0.00046	0.00331				0.00377
SSE	0.00012	0.00011	0.00126				0.00149
SSW		0.00023	0.00023				0.00046
SW	0.00023	0.00091	0.00126				0.00240
W	0.00023	0.00206	0.00640				0.00869
WNW		0.00080	0.00640				0.00720
WSW	0.00023	0.00114	0.00560				0.00697
Sum	0.00117	0.01051	0.05139				0.06307

Table 2.5-6 (cont.)

From 2/1/2014 To 1/31/2015

Stability Class D **Wind Speed (mph)**

Direction	< 3	4 - 7	8 - 12	13-18	19 - 24	> 24	Row Total
E		0.00811	0.01382	0.00788	0.00034		0.03015
ENE		0.00411	0.00902	0.00514	0.00057		0.01884
ESE	0.00012	0.00879	0.02935	0.02250	0.00263		0.06339
N		0.00434	0.01485	0.01976	0.00845	0.00411	0.05151
NE		0.00434	0.00742	0.00617	0.00148		0.01942
NNE	0.00023	0.00457	0.01028	0.01016	0.00320	0.00057	0.02901
NNW		0.00377	0.01165	0.01450	0.00799	0.00754	0.04545
NW		0.00445	0.01085	0.01142	0.00480	0.00297	0.03449
S		0.00023	0.00069	0.00057			0.00148
SE	0.00035	0.00343	0.00731	0.00708	0.00286	0.00011	0.02114
SSE		0.00080	0.00148	0.00114	0.00023		0.00365
SSW	0.00035	0.00148	0.00126	0.00091	0.00023		0.00423
SW	0.00035	0.00411	0.00274	0.00286	0.00126	0.00069	0.01200
W	0.00035	0.01496	0.05413	0.07686	0.03757	0.02204	0.20592
WNW	0.00012	0.00811	0.02318	0.03026	0.01313	0.00320	0.07801
WSW	0.00047	0.00914	0.01256	0.02535	0.02159	0.02844	0.09754
Sum	0.00234	0.08474	0.21060	0.24258	0.10633	0.06967	0.71625

Table 2.5-6 (cont.)

From 2/1/2014 To 1/31/2015

Stability Class E **Wind Speed (mph)**

Direction	< 3	4 - 7	8 - 12	13-18	19 - 24	> 24	Row Total
E	0.00035	0.00251	0.00423				0.00709
ENE	0.00023	0.00228	0.00148				0.00400
ESE		0.00388	0.00845				0.01233
N		0.00160	0.00046				0.00206
NE		0.00217	0.00126				0.00343
NNE	0.00023	0.00308	0.00148				0.00480
NNW	0.00012	0.00183	0.00091				0.00286
NW		0.00217	0.00091				0.00308
S		0.00069					0.00069
SE	0.00047	0.00228	0.00080				0.00355
SSE		0.00091	0.00023				0.00114
SSW	0.00035	0.00057	0.00034				0.00127
SW	0.00023	0.00320	0.00023				0.00366
W	0.00094	0.00640	0.00662				0.01396
WNW	0.00047	0.00434	0.00263				0.00744
WSW	0.00059	0.00445	0.00183				0.00687
Sum	0.00398	0.04237	0.03186				0.07822

Table 2.5-6 (cont.)

From 2/1/2014 To 1/31/2015

Stability Class F **Wind Speed (mph)**

Direction	< 3	4 - 7	8 - 12	13-18	19 - 24	> 24	Row Total
E	0.00152	0.00160					0.00312
ENE	0.00105	0.00114					0.00220
ESE	0.00105	0.00183					0.00288
N	0.00187	0.00148					0.00336
NE	0.00082	0.00126					0.00208
NNE	0.00129	0.00069					0.00197
NNW	0.00129	0.00126					0.00254
NW	0.00105	0.00274					0.00380
S	0.00105	0.00240					0.00345
SE	0.00152	0.00114					0.00267
SSE	0.00246	0.00160					0.00406
SSW	0.00199	0.00171					0.00370
SW	0.00211	0.00308					0.00519
W	0.00269	0.00388					0.00658
WNW	0.00187	0.00400					0.00587
WSW	0.00223	0.00320					0.00542
Sum	0.02589	0.03301					0.05890

Table 2.5-7: Black Thunder SODAR Results

Time Period (Filtered)	Number of Data Points	Average Mixing / Inversion Height
Morning (2 am – 6 am)	193	641 meters
Afternoon (12 pm – 4 pm)	152	1,052 meters

Table 2.5-8: Particulate Matter (PM) Monitoring History at Douglas, Wyoming

Statistic	2013	2014	2015
Valid Days PM_{10}	361	365	180
Annual Mean PM_{10}	10.1	9.2	8.1
Maximum 24-Hour Average PM_{10}	99	36	71
2^{nd} High 24-Hour Average PM_{10}	39	32	43
WAAQS 2^{nd} High 24-Hour Average PM_{10}	150	150	150
Valid Days $PM_{2.5}$	357	364	180
Annual Mean $PM_{2.5}$	3.3	2.3	2.5
Maximum 24-Hour Average $PM_{2.5}$	10.7	15.8	11.4
98^{th} Percentile 24-Hour Average $PM_{2.5}$	8.2	8.0	6.3
WAAQS 98^{th} Percentile 24-Hour Average $PM_{2.5}$	12	12	12

Source: EPA AirData, 2015

Table 2.5-9: Primary and Secondary Standards for each Criteria of Pollutants

Pollutant	Averaging Interval and Statistic	NAAQS Primary Standard	NAAQS Secondary Standard	WAAQS
PM_{10}	Annual Average	--	--	50 $\mu g/m^3$
	4th High 24-Hr Maximum	150 $\mu g/m^3$	150 $\mu g/m^3$	150 $\mu g/m^3$
$PM_{2.5}$	Annual Average	12 $\mu g/m^3$	15 $\mu g/m^3$	12 $\mu g/m^3$
	24-Hr High	35 $\mu g/m^3$	35 $\mu g/m^3$	35 $\mu g/m^3$
O_3	Annual 4th Highest Daily 8-Hr Average	70 ppb	70 ppb	.070 ppm
NO_2	Annual Average	53 ppb	53 ppb	53 ppb
	98th Percentile of Daily 1-Hr Highs	100 ppb	--	100 ppb
SO_2	Annual Average	--	--	--
	24-Hr	--	--	--
	3-Hr	--	0.5 ppm	0.5 ppm
	99th Percentile of Daily 1-Hr Highs	75 ppb	--	75 ppb
CO	8-Hr High	9 ppm	--	10 mg/m^3
	1-Hr High	35 ppm	--	40 mg/m^3
Pb	Rolling 3-Month Average	0.15 $\mu g/m^3$	0.15 $\mu g/m^3$	0.15 $\mu g/m^3$

Table 2.5-10: Maximum Allowable PSD Increments for Class I and Class II Areas

Pollutant	Averaging Interval and Statistic	PSD Class I Increment	PSD Class II Increment
PM_{10}	Annual Average	4 µg/m^3	17 µg/m^3
	4th High 24-Hr Maximum	8 µg/m^3	30 µg/m^3
$PM_{2.5}$	Annual Average	1 µg/m^3	4 µg/m^3
	24-Hr High	2 µg/m^3	9 µg/m^3
O_3	Annual 4th Highest Daily 8-Hr Average	--	--
NO_2	Annual Average	2.5 µg/m^3	25 µg/m^3
	98th Percentile of Daily 1-Hr Highs	--	--
SO_2	Annual Average	2 µg/m^3	20 µg/m^3
	24-Hr	5 µg/m^3	91 µg/m^3
	3-Hr	25 µg/m^3	512 µg/m^3
	99th Percentile of Daily 1-Hr Highs	--	--
CO	8-Hr High	--	--
	1-Hr High	--	--

Table 2.5-11: Casper Wind Speed and Direction Summary Statistics

Statistic	Average Wind Speed (mph)	Unit Vector Average Wind Direction (°)	Wind Speed Vector Average Wind Direction (°)
1997 through 2013	10.9	249.4	239.4
Baseline Year	11.2	254.0	244.5

Table 2.5-12: χ^2 Test for Annualized Wind Speed Distributions

Wind Speeds- Casper LT/ST Frequency x 8,760				
mph	**17 Yr WS**	**1Yr WS**	**$(LT-ST)^2/LT$**	**Chi-Square**
0-3	455	501	4.691	39.70
4-7	2082	1905	14.908	$\chi^2_{0.95}(6)=12.59$
8-12	2427	2366	1.548	Reject H_o
13-18	1949	2139	18.541	p-value=0.000
19-24	774	773	0.002	Min Count=455
>24	509	511	0.015	Phi-value=0.07
Calm	564	564	0.000	Adj: Do Not Reject

Table 2.5-13: χ^2 Test for Annualized Wind Direction Distributions

Wind Directions- Casper LT/ST Frequency x 8,760				
Direection	**17 Yr WS**	**1Yr WS**	**$(LT-ST)^2/LT$**	**Chi-Square**
N	389	415	1.755	48.96
NNE	562	628	7.800	$\chi^2_{0.95}(6)=26.30$
NE	428	422	0.086	Reject H_o
ENE	353	300	7.780	p-value=0.000
E	506	483	1.053	Min Count=68
ESE	178	185	0.224	Phi-value=0.07
SE	84	83	0.001	Adj: Do Not Reject
SSE	68	75	0.777	
S	179	202	3.038	
SSW	873	772	11.720	
SW	1770	1770	0.000	
WSW	1139	1076	3.471	
W	729	765	1.791	
WNW	358	371	0.461	
NW	294	341	7.549	
NNW	286	306	1.458	
Calm	564	564	0.000	

Table 2.5-14: χ^2 Test for Wind Direction with Smaller Scaling Factor

Wind Directions- Casper LT/ST Frequency x 8,760				
Direection	**17 Yr WS**	**1Yr WS**	**$(LT-ST)^2/LT$**	**Chi-Square**
N	44	47	0.200	5.59
NNE	64	72	0.890	$\chi^2_{0.95}(6)=26.30$
NE	49	48	0.010	Can't Reject H_o
ENE	40	34	0.888	p-value=0.992
E	58	55	0.120	Min Count=8
ESE	20	21	0.026	Phi-value=0.07
SE	10	9	0.000	Adj: Confirm
SSE	8	9	0.089	
S	20	23	0.347	
SSW	100	88	1.338	
SW	202	202	0.000	
WSW	130	123	0.396	
W	83	87	0.204	
WNW	41	42	0.053	
NW	34	39	0.862	
NNW	33	35	0.166	
Calm	64	64	0.000	

Table 2.5-15: χ^2 Test for Wind Speed with Smaller Scaling Factor

Wind Speeds- Casper LT/ST Frequency x 1,000				
mph	**17 Yr WS**	**1Yr WS**	**$(LT-ST)^2/LT$**	**Chi-Square**
0-3	52	57	0.535	4.53
4-7	238	218	1.702	$\chi^2_{0.95}(6)=12.59$
8-12	277	270	0.177	Can't Reject H_o
13-18	222	244	2.117	p-value=0.605
19-24	88	88	0.000	Min Count=52
>24	558	58	0.002	Phi-value=0.07
Calm	64	64	0.000	Adj: Confirm

Table 2.5-16: Summary of Statistical Analysis of Freq. Distributions at Casper

17-Yr vs. 1-Yr Frequency Distributions	Statistical Method						Overall Conclusion
	χ^2 at 8,760 hrs.	∅-Coeff.	χ^2 at 1,000 hrs.	∅-Coeff.	Linear Regress. R^2	p-value for R^2	
Wind Speed	48.96	0.07	5.59	0.07	0.983	0.000	No Statistical Differnce
Wind Direction	39.70	0.07	4.53	0.07	0.988	0.000	No Statistical Differnce
Joint Wind Speed and Wind Direction	N/A	N/A	N/A	N/A	0.979	0.000	No Statistical Differnce

FIGURES

Figure 2.5-1: NWS and Coal Mine Meteorological Stations

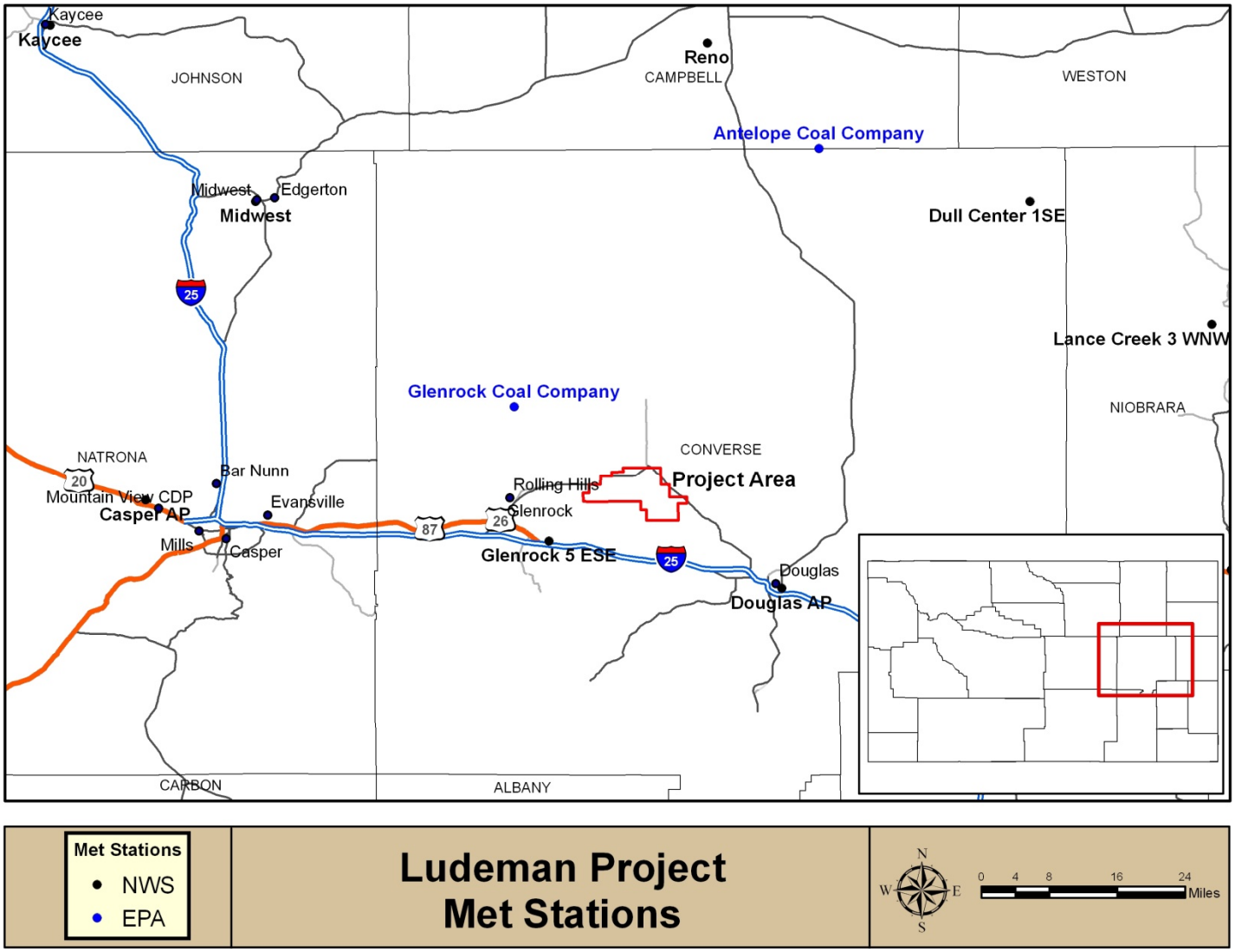

Figure 2.5-2: Regional Average Monthly Temperatures

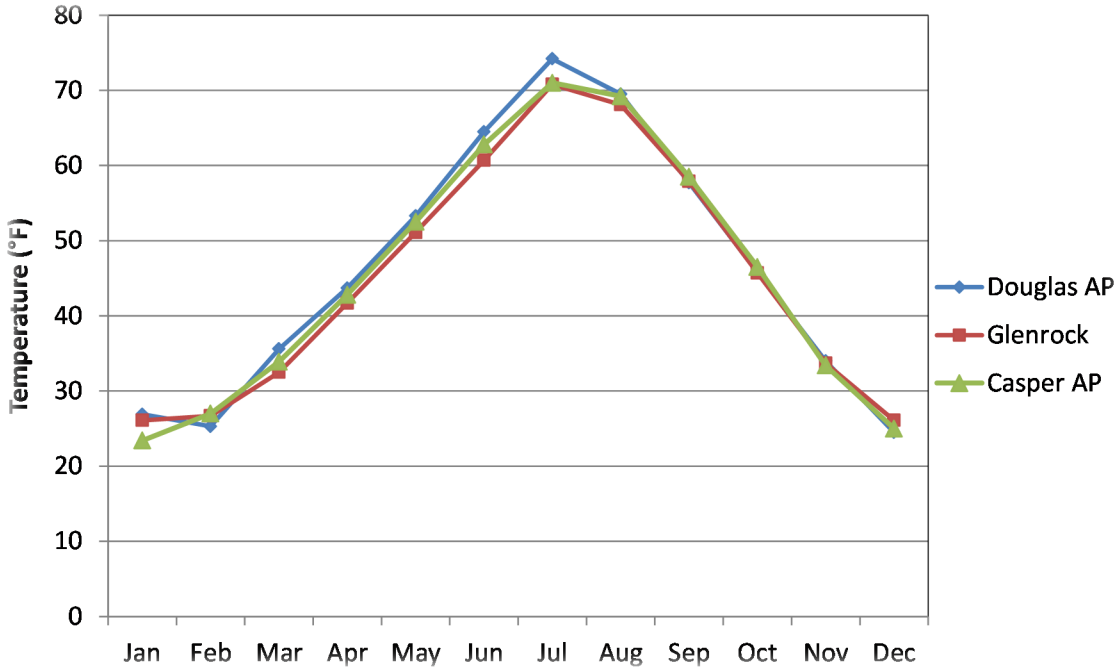

Figure 2.5-3: Regional Annual Average Minimum Temperatures

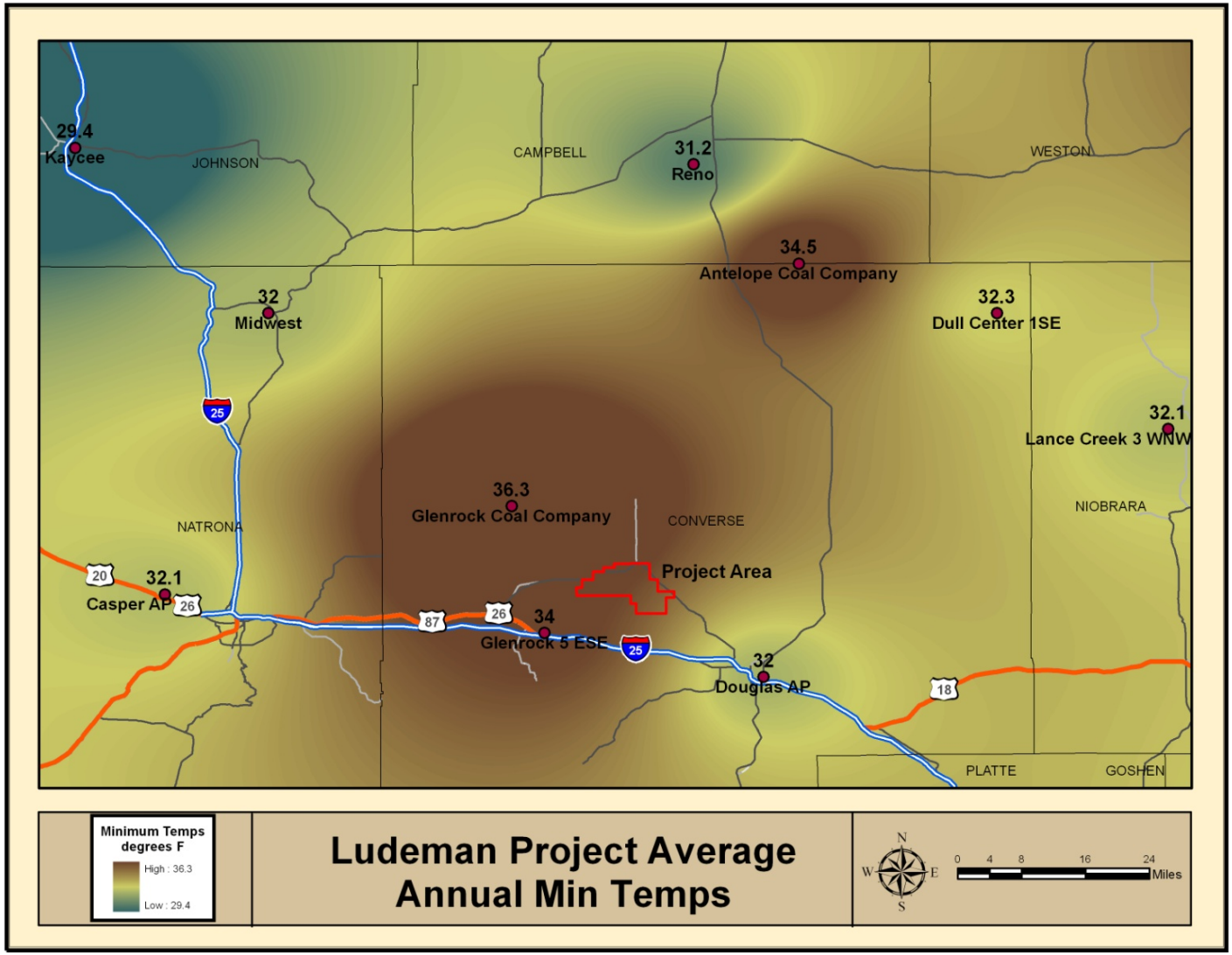

Figure 2.5-4: Regional Annual Average Maximum Temperatures

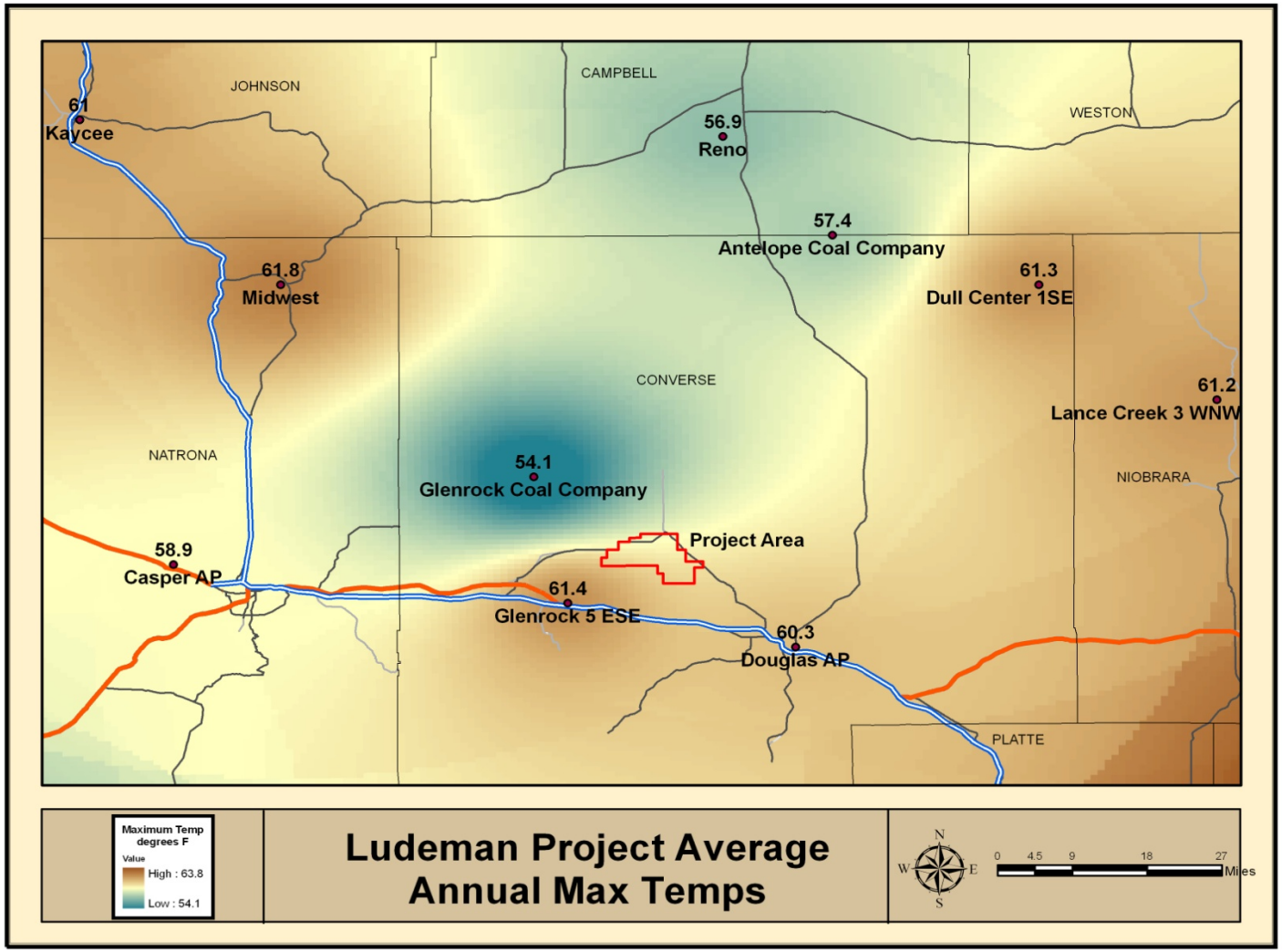

Figure 2.5-5: GCC and Douglas AP Seasonal Diurnal Temperature Variation

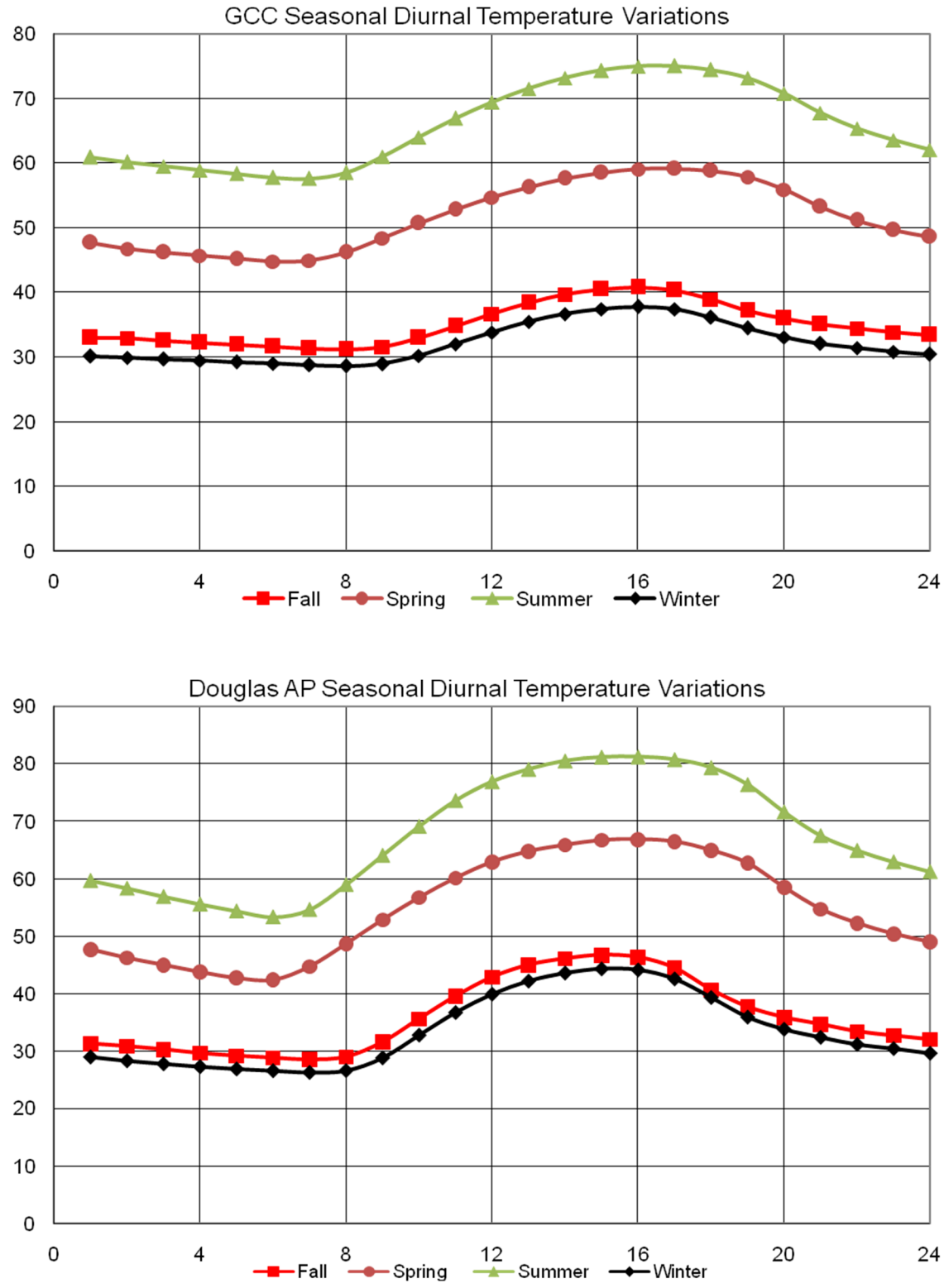

Figure 2.5-6: Monthly Relative Humidity Statistics for Region (NCDC, 2015)

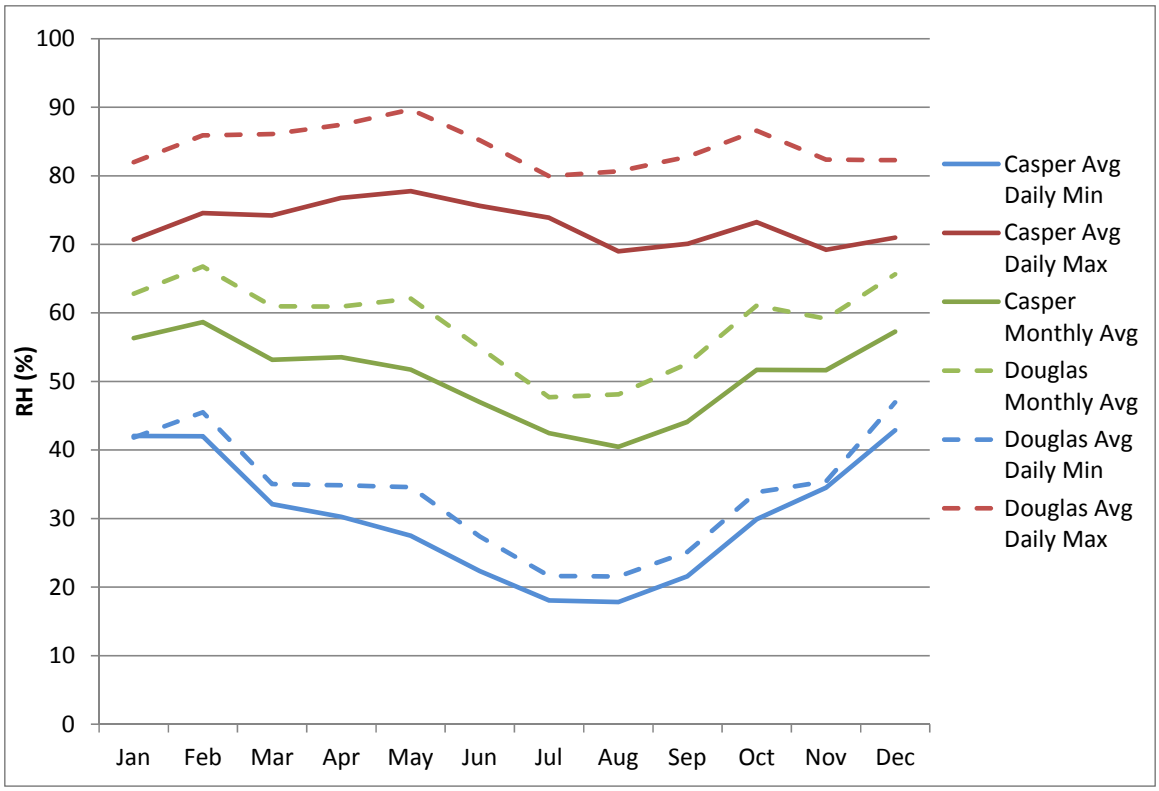

Figure 2.5-7: Mean Monthly and Hourly RH for Casper Airport (WRDS, 2007)

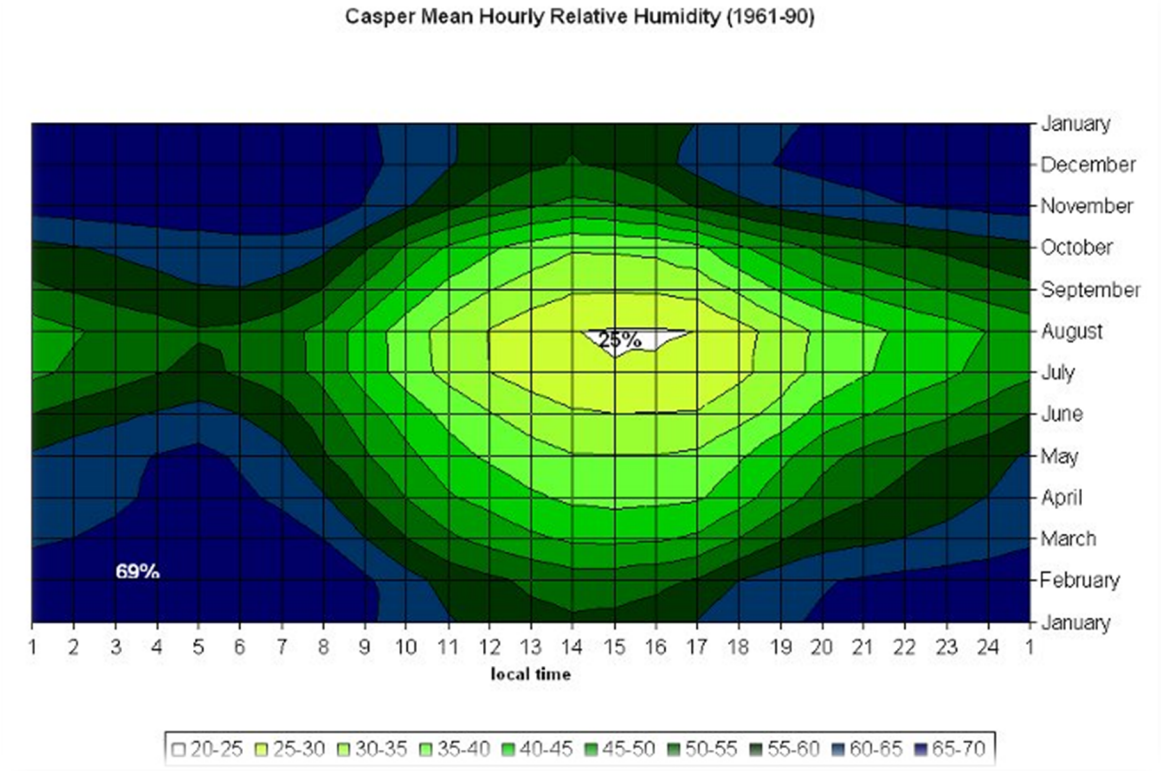

Figure 2.5-8: Regional Annual Average Precipitation

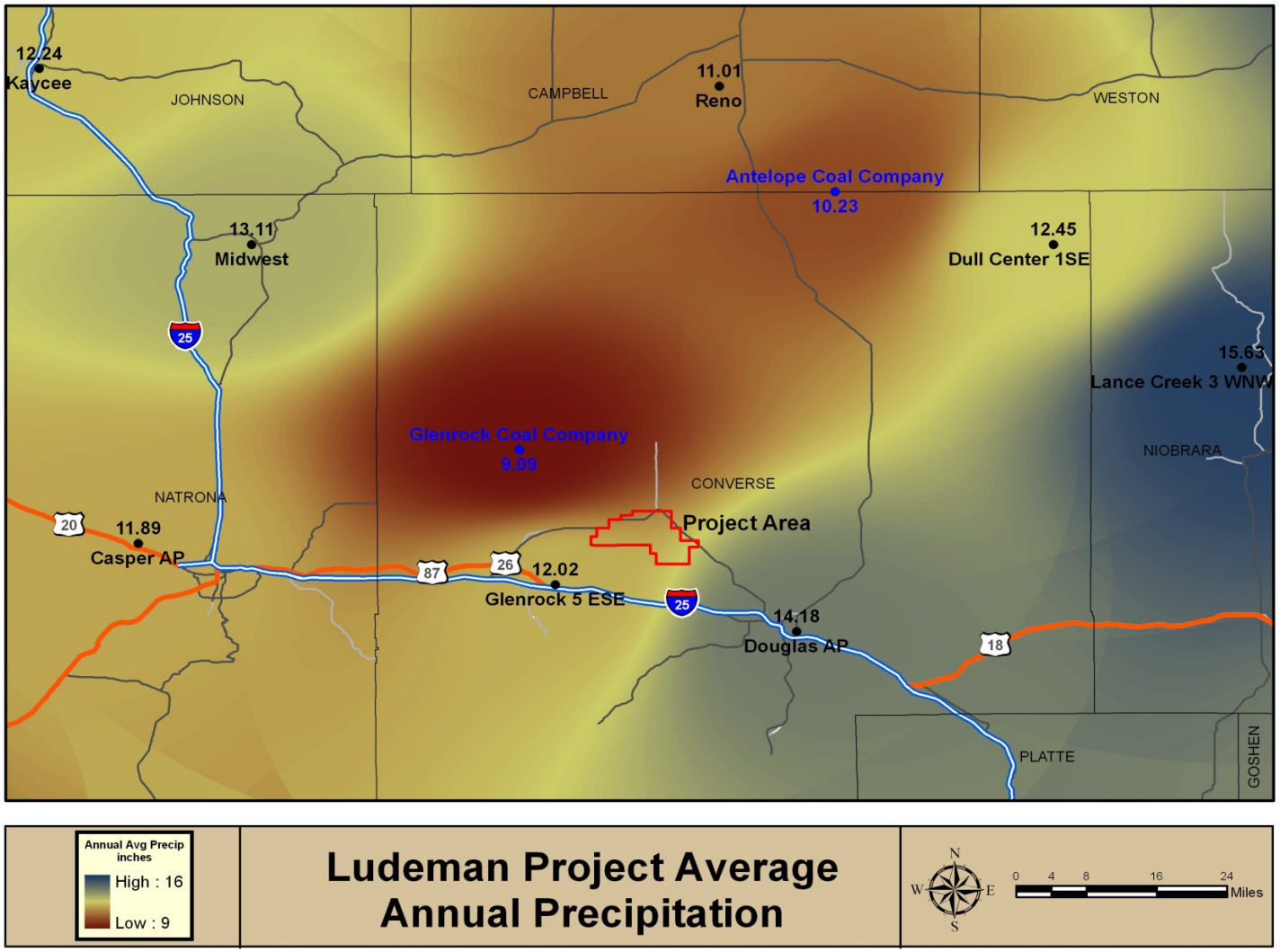

Figure 2.5-9: NWS Station Monthly Precipitation Averages (NCDC, 2007)

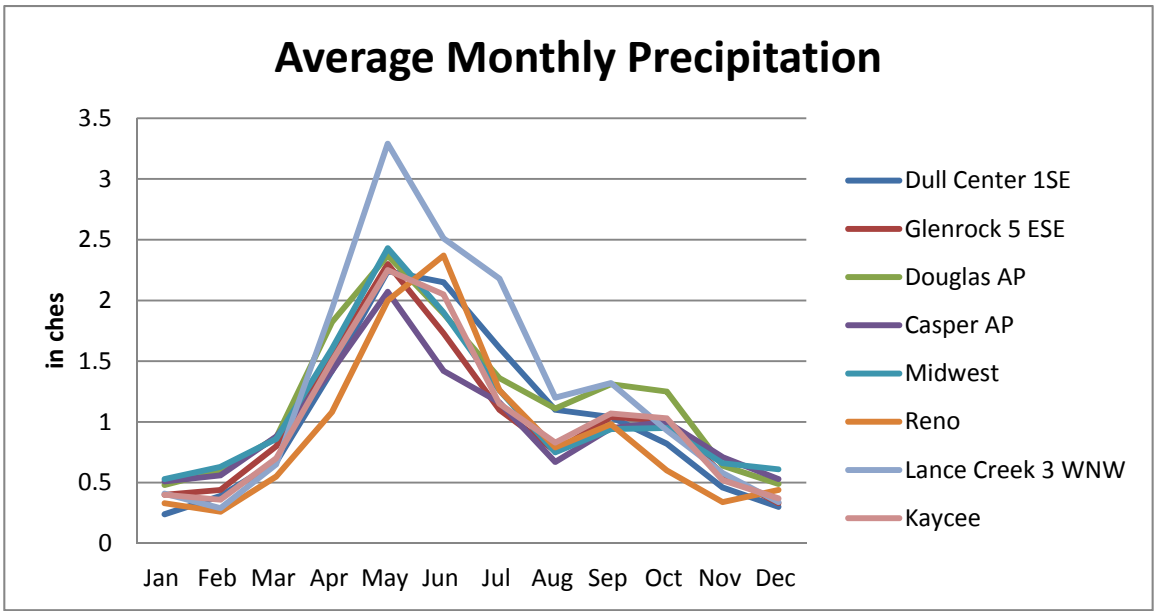

Figure 2.5-10: NWS Station Monthly Snowfall Averages (NCDC, 2007)

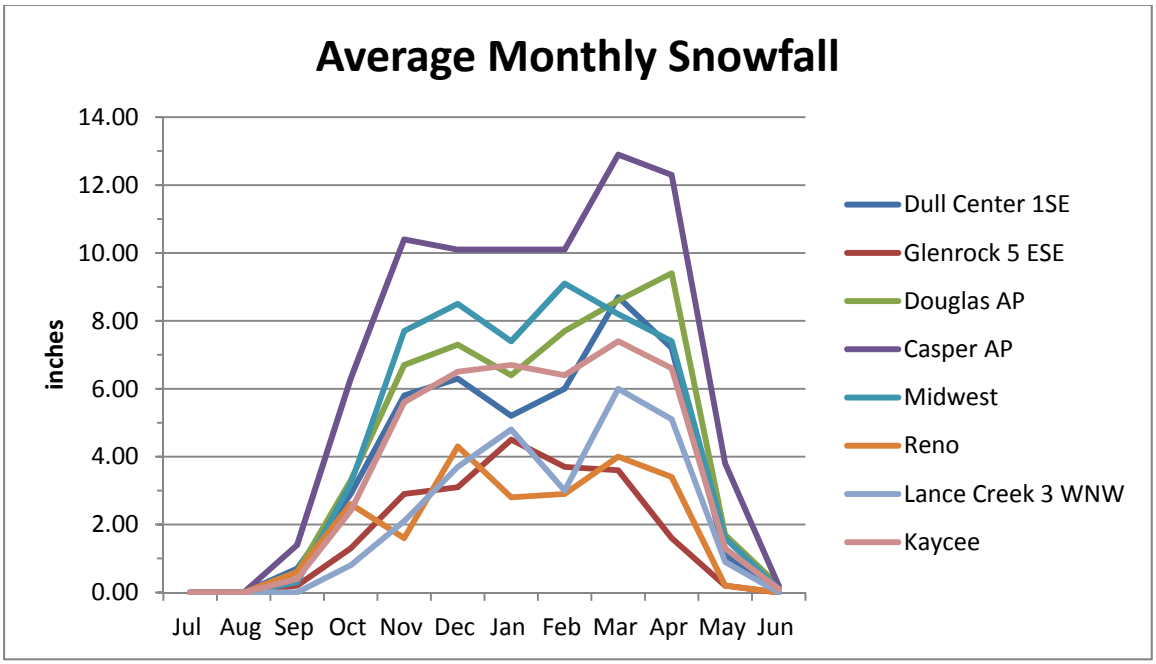

Figure 2.5-11: Regional Annual Average Snowfall

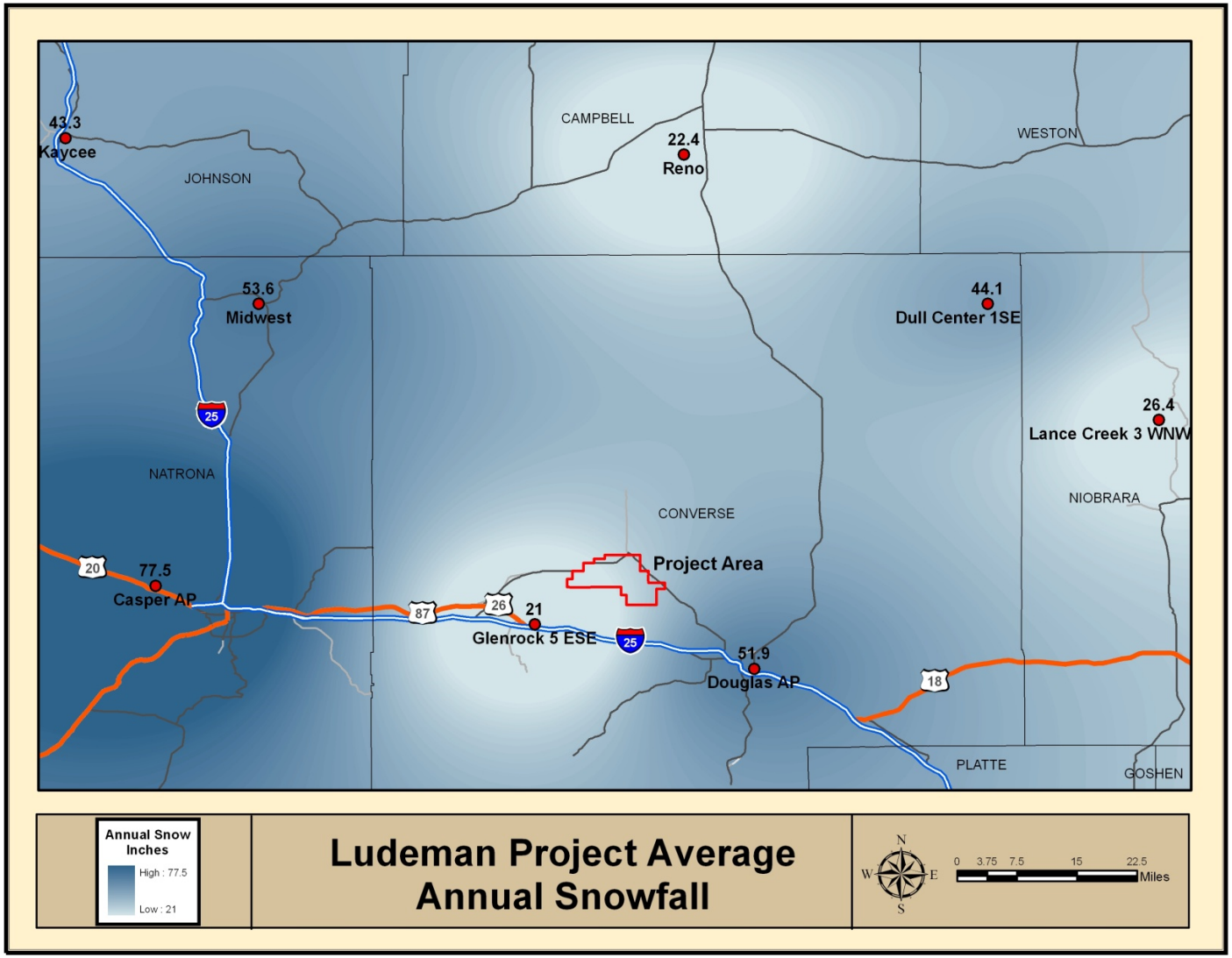

Figure 2.5-12: Regional Wind Speeds by Month (WRCC 2015)

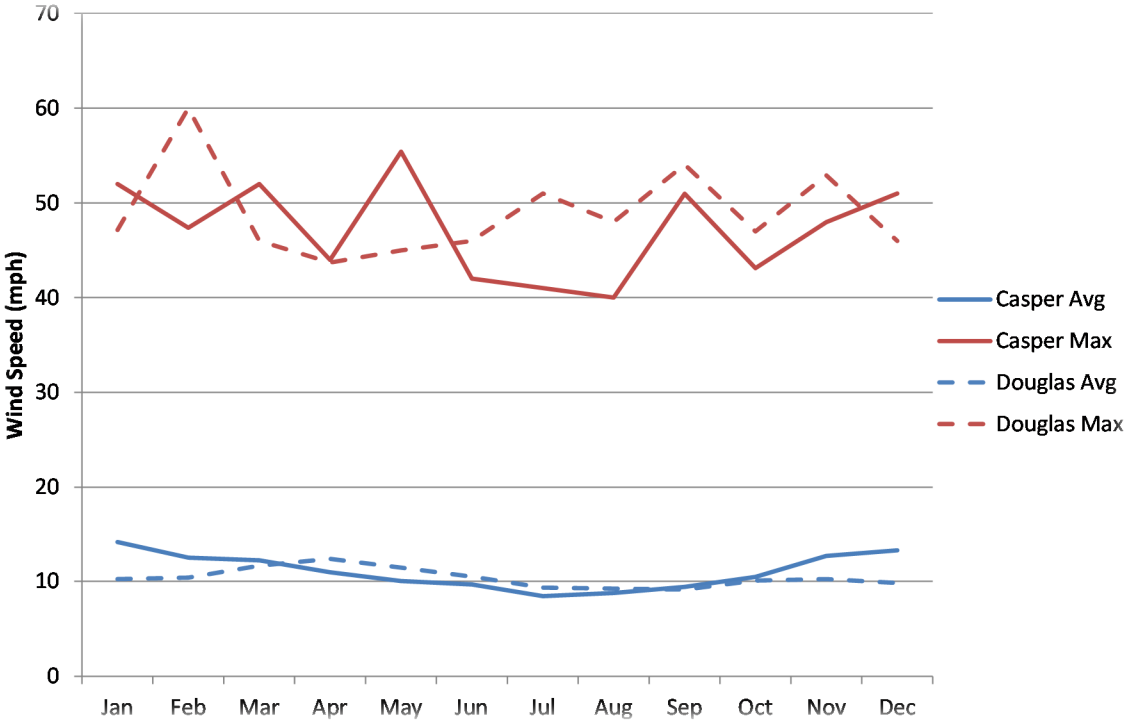

Figure 2.5-13: Regional Wind Roses (WRCC 2015)

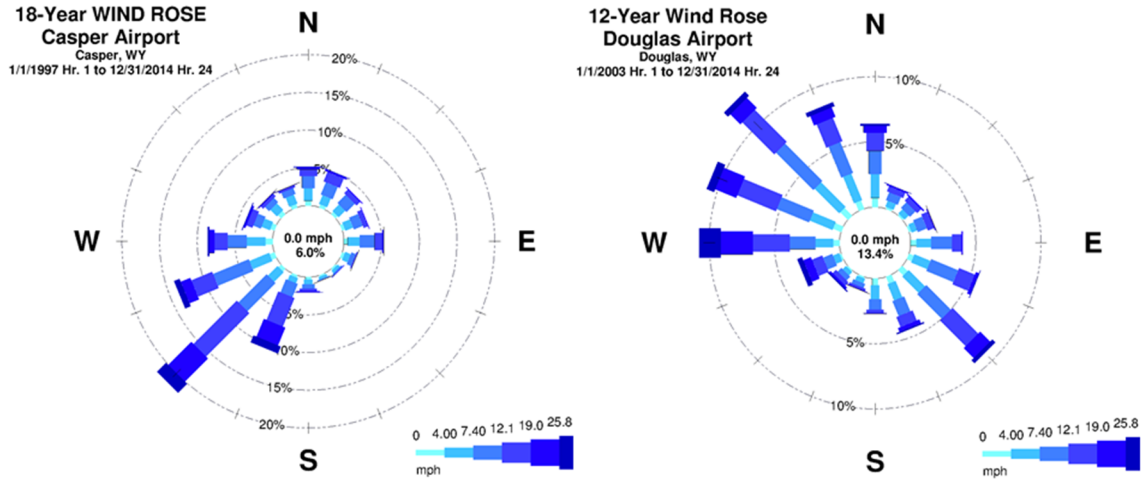

Figure 2.5-14: Casper Cooling, Heating, and Growing Degree Days (WRCC 2007)

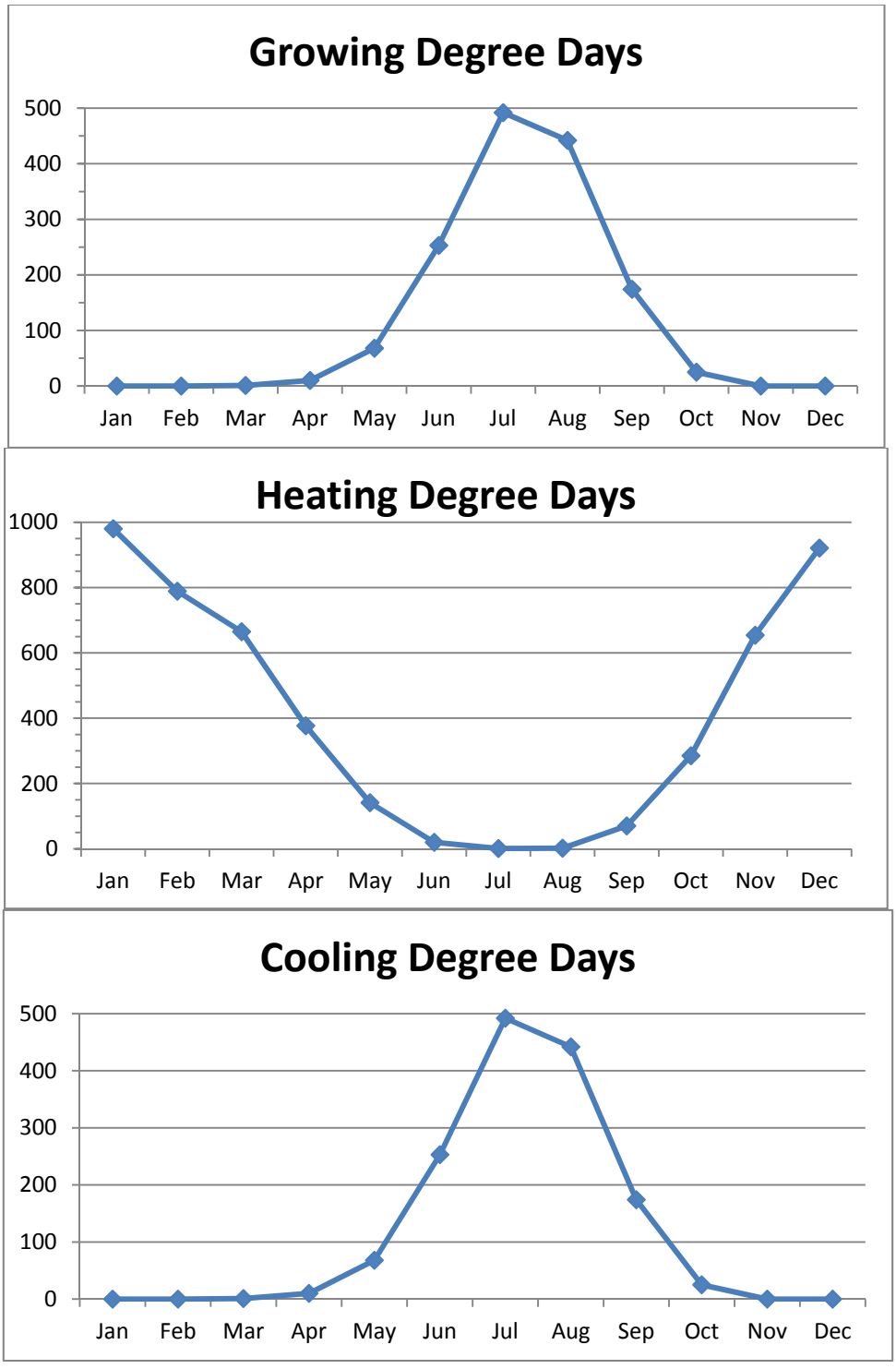

Figure 2.5-15: Ludeman Site Monthly Temperature Statistics

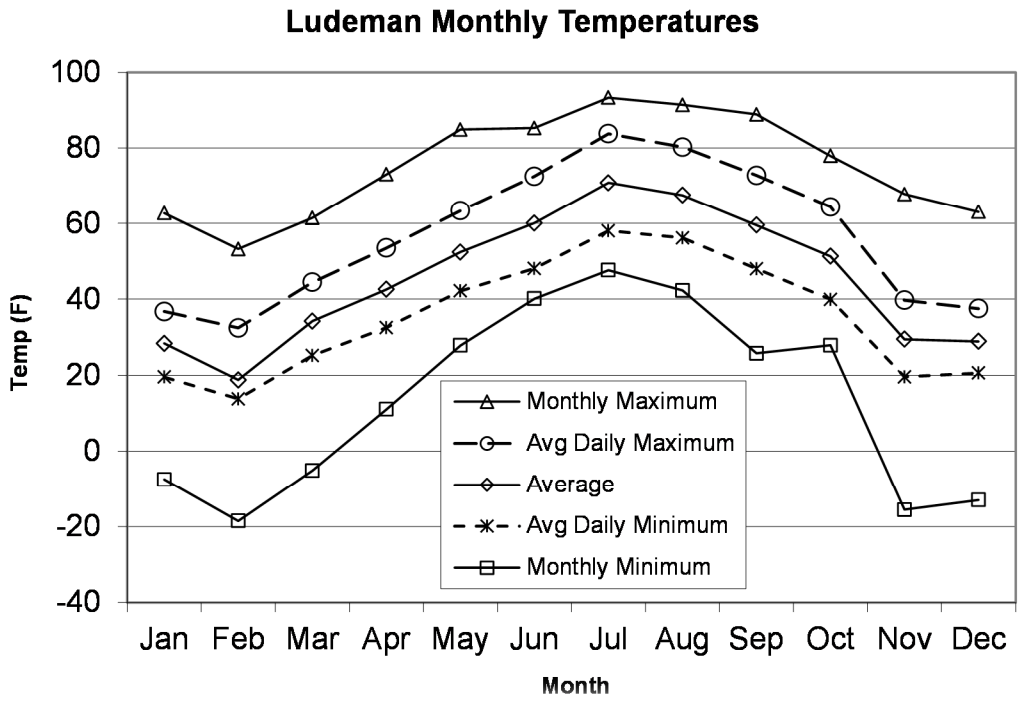

Figure 2.5-16: On-Site Temperatures vs. Nearby Met Stations

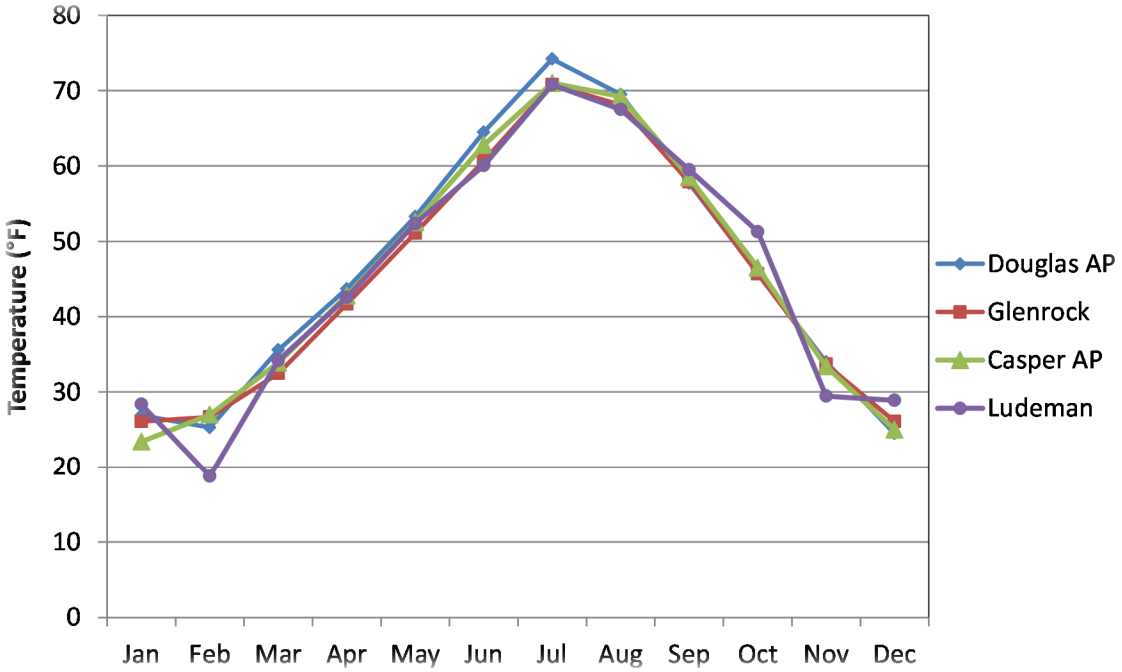

Figure 2.5-17: Ludeman Diurnal Temperature Profiles

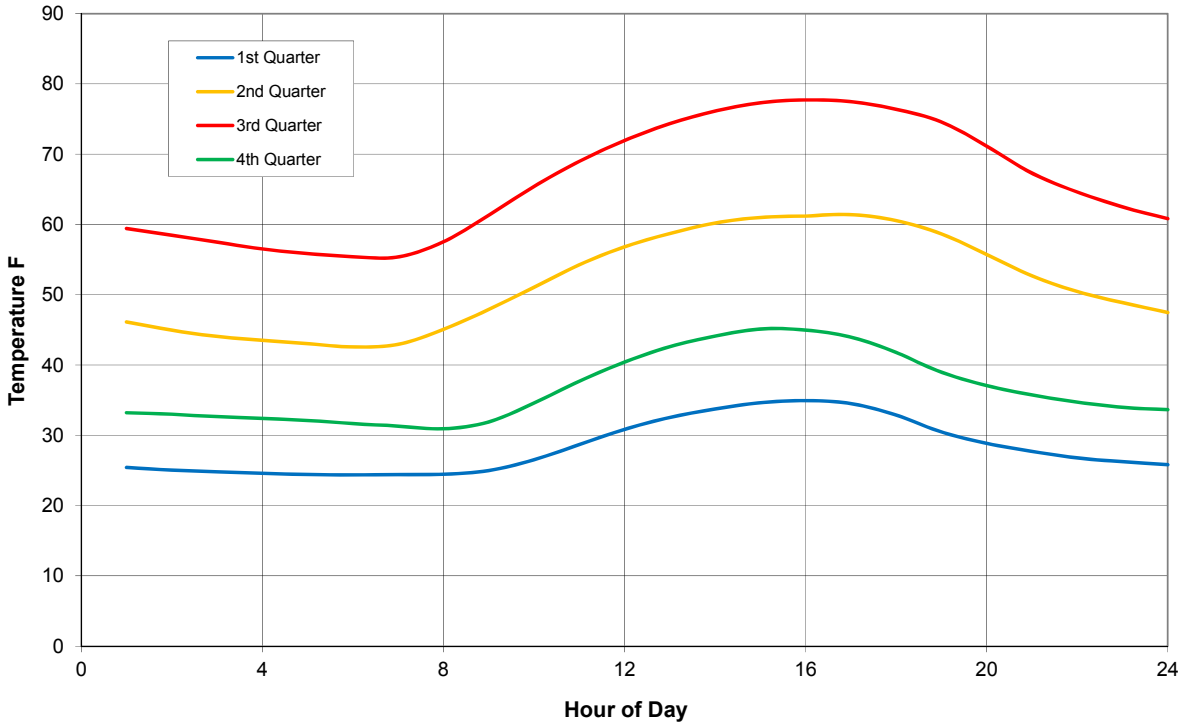

Figure 2.5-18: Ludeman Site Baseline Year and Quarterly Wind Roses

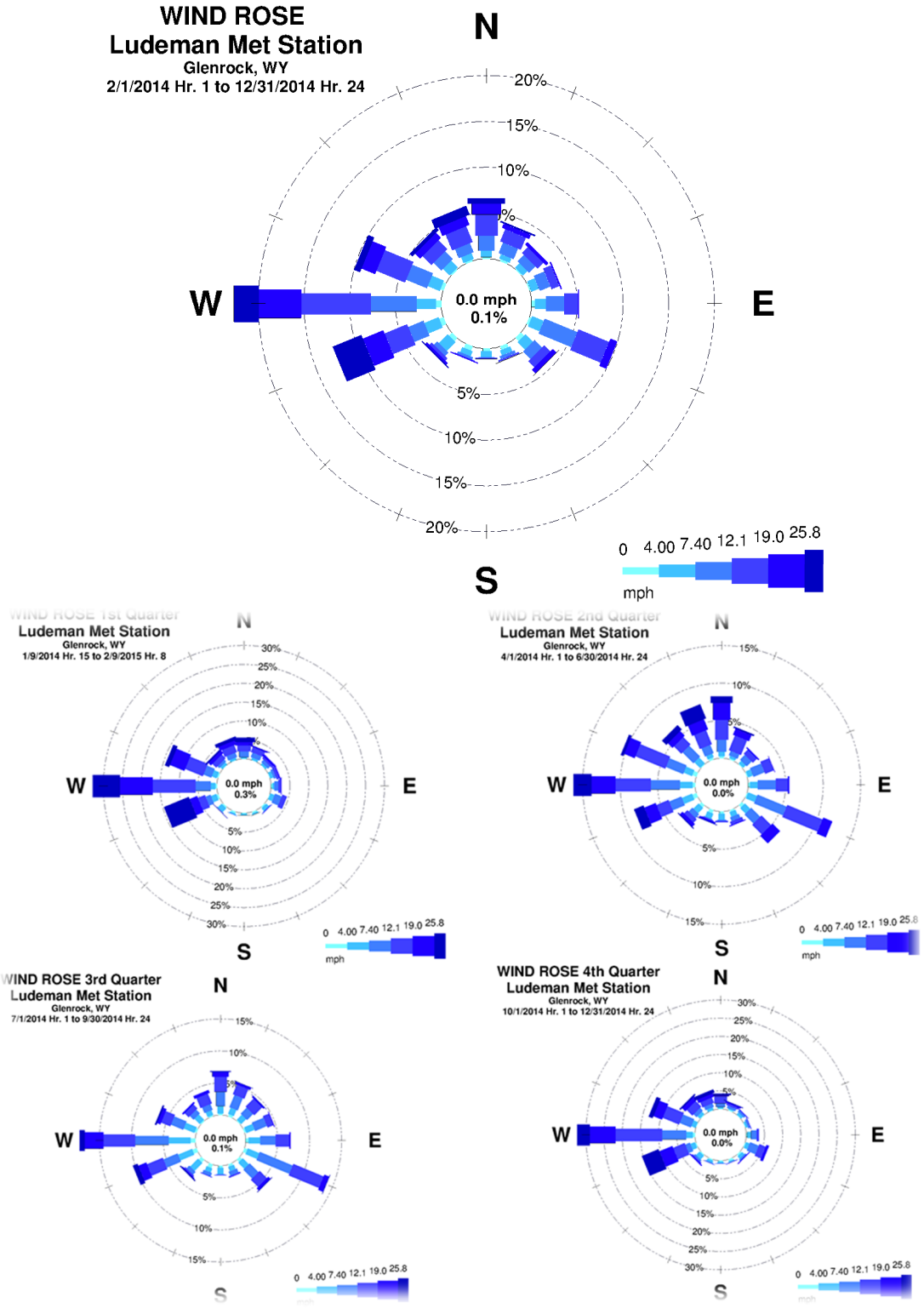

Figure 2.5-19: Comparison of Douglas AP and Ludeman Site Wind Roses

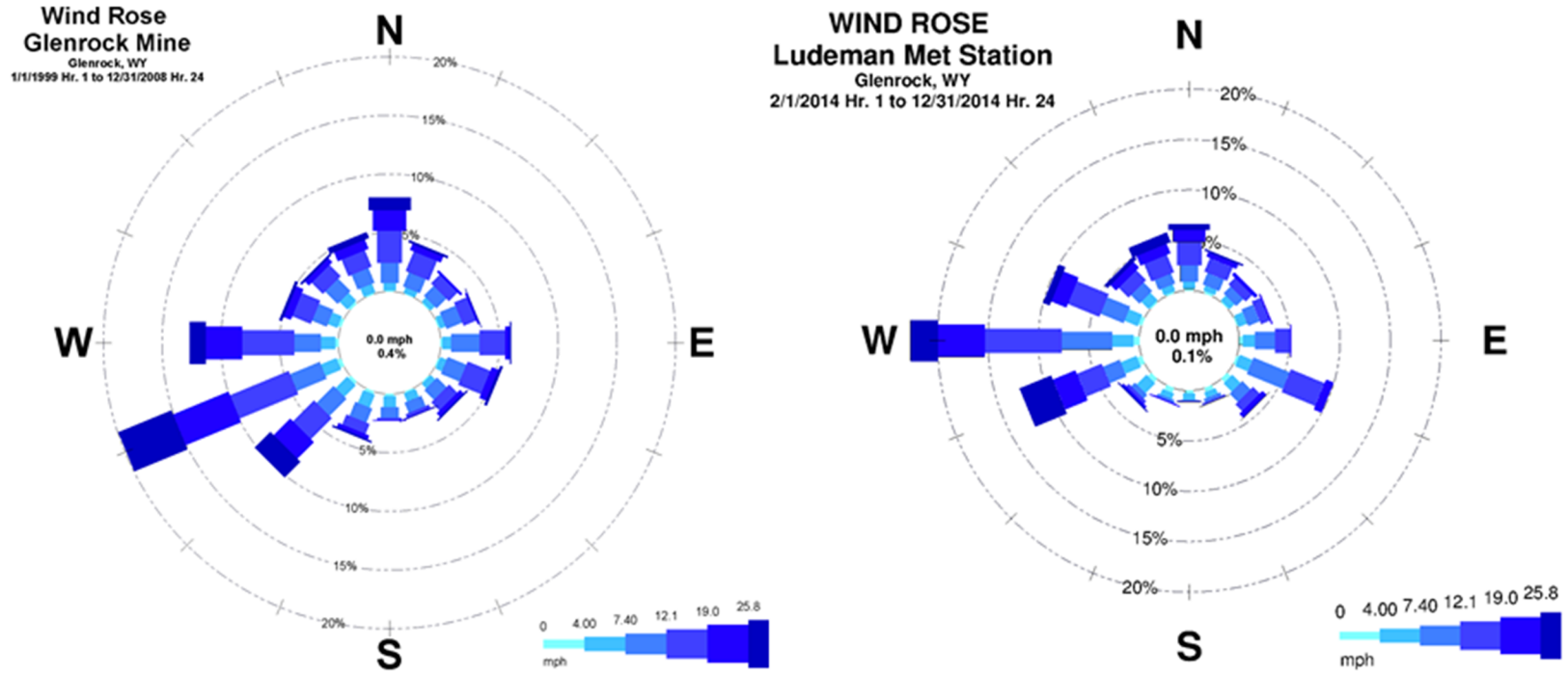

Figure 2.5-20: Comparison of Douglas AP and Ludeman Site Wind Roses

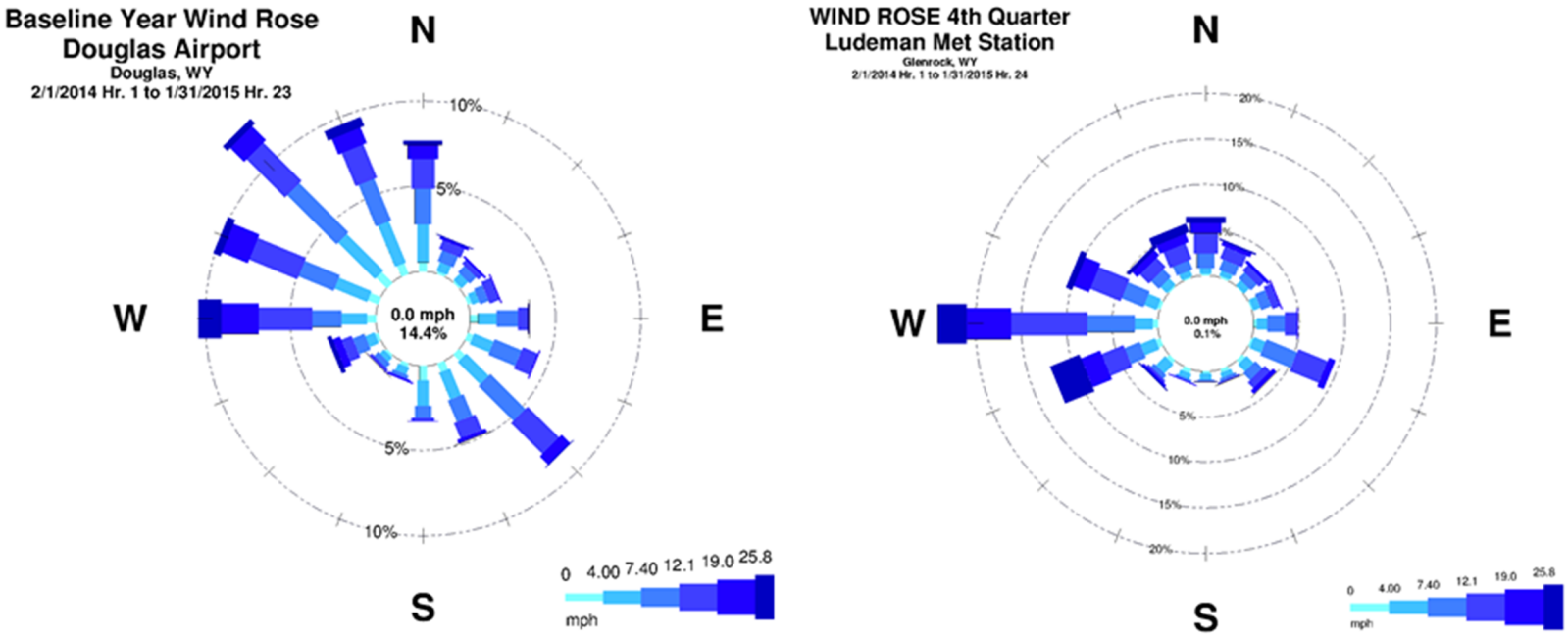

Figure 2.5-21: Ludeman Monthly Maximum and Average Wind Speed Averages

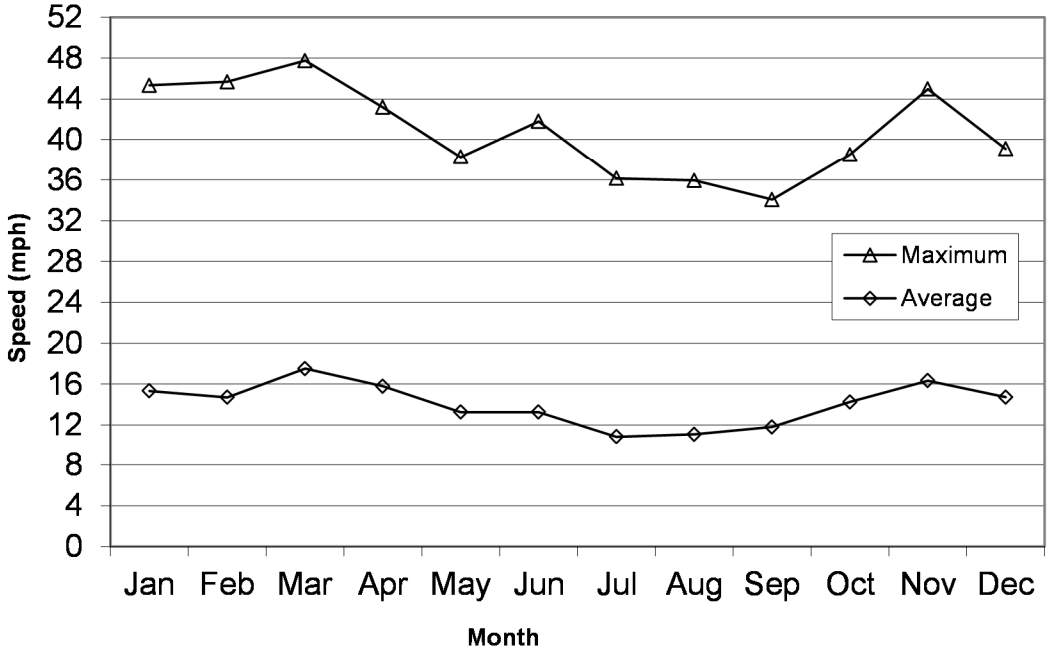

Figure 2.5-22: Ludeman Diurnal Wind Speeds

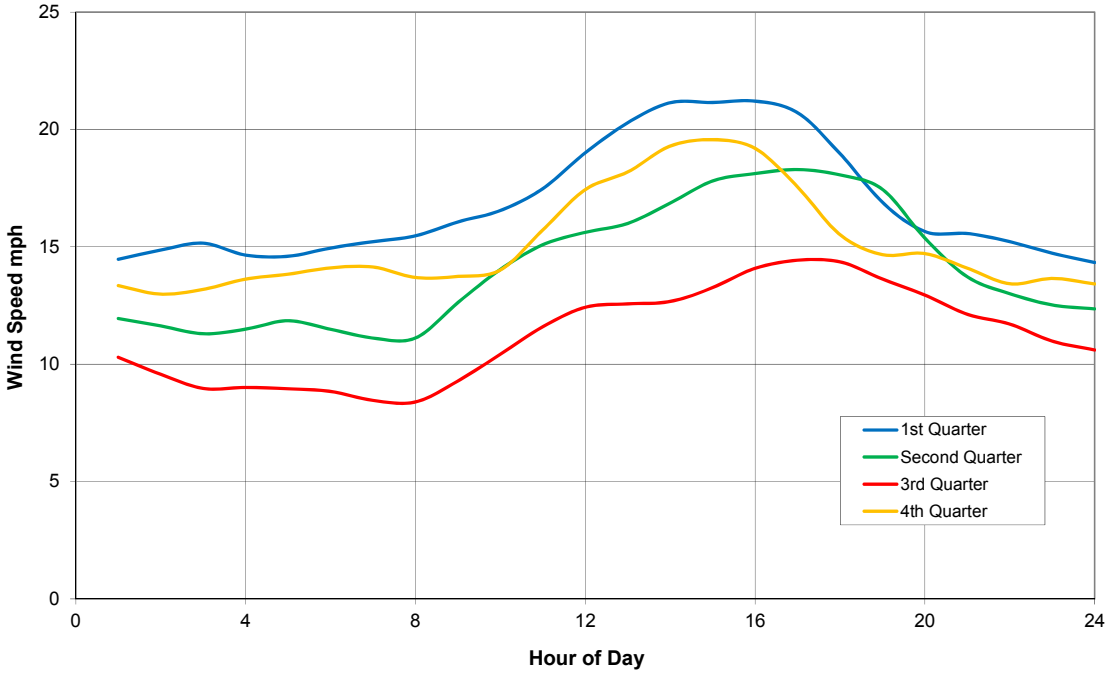

Figure 2.5-23: Ludeman Wind Speed Frequency Distribution

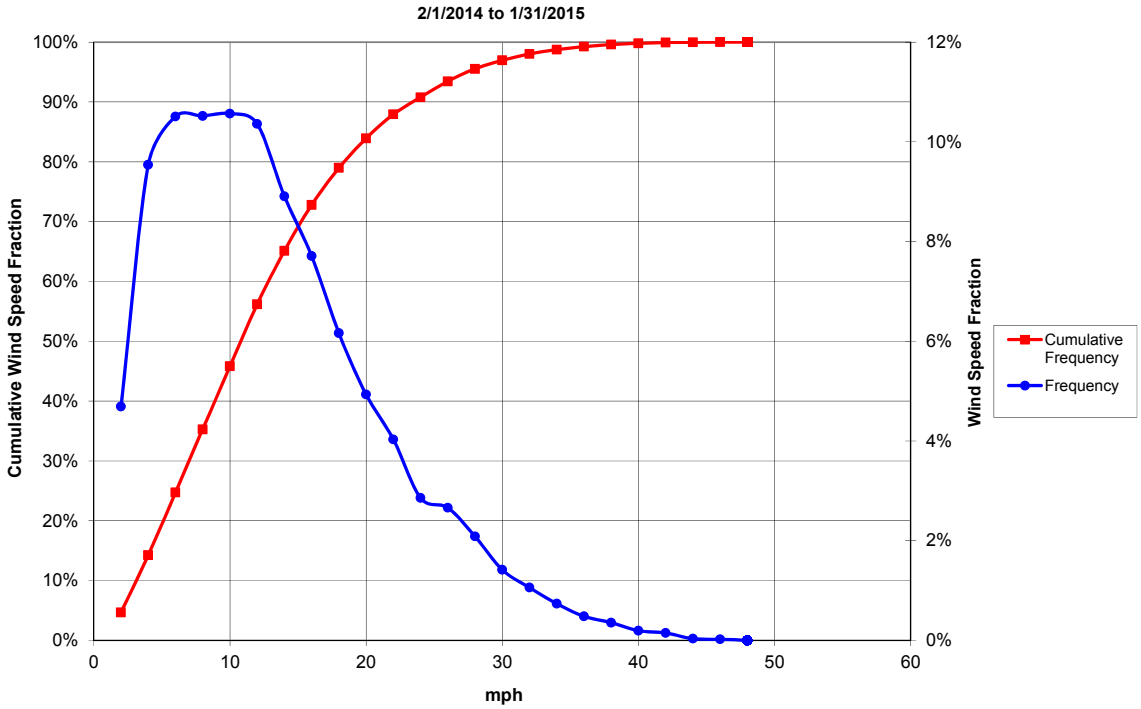

Figure 2.5-24: Ludeman Baseline Year Precipitation

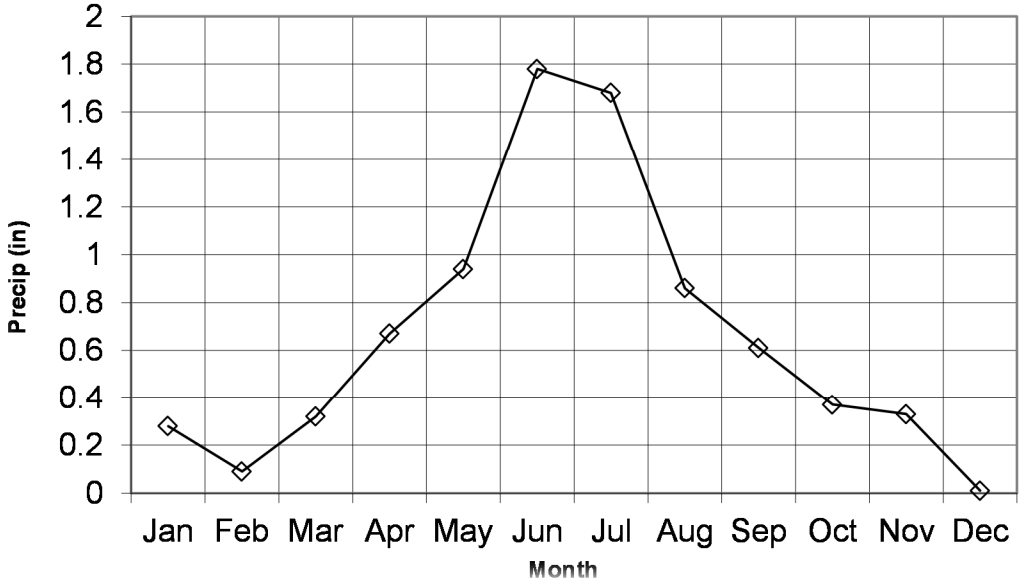

Figure 2.5-25: Ludeman Monthly RH

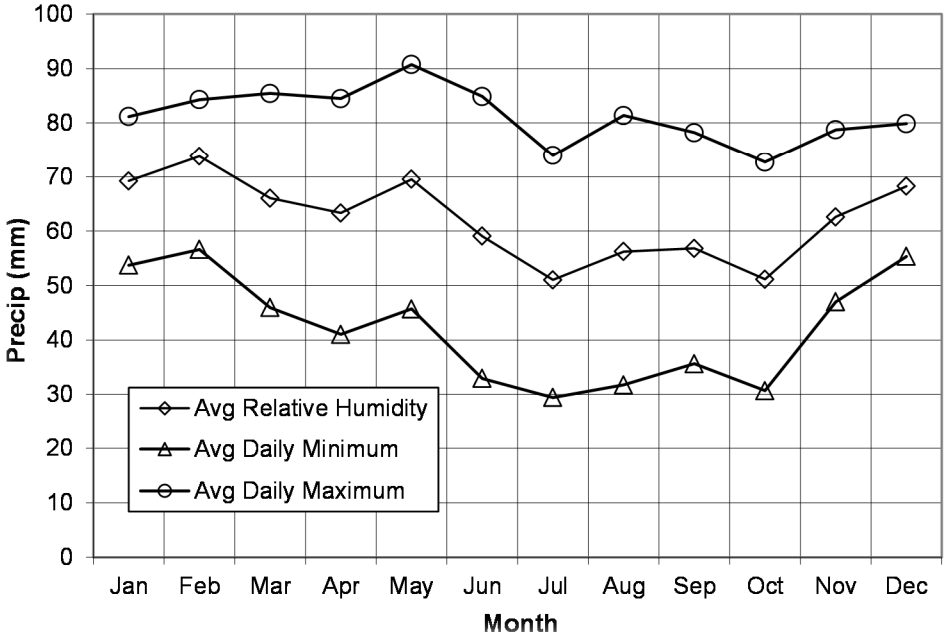

Figure 2.5-26: Ludeman Monthly RH

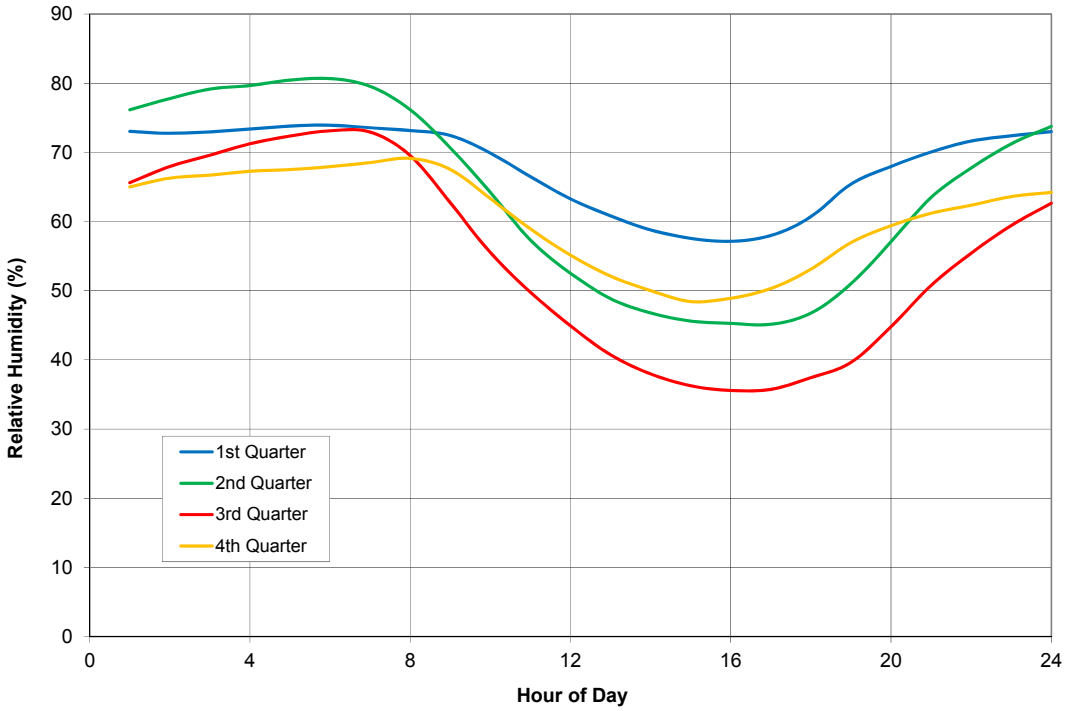

Figure 2.5-27: Ludeman Monthly Solar Radiation

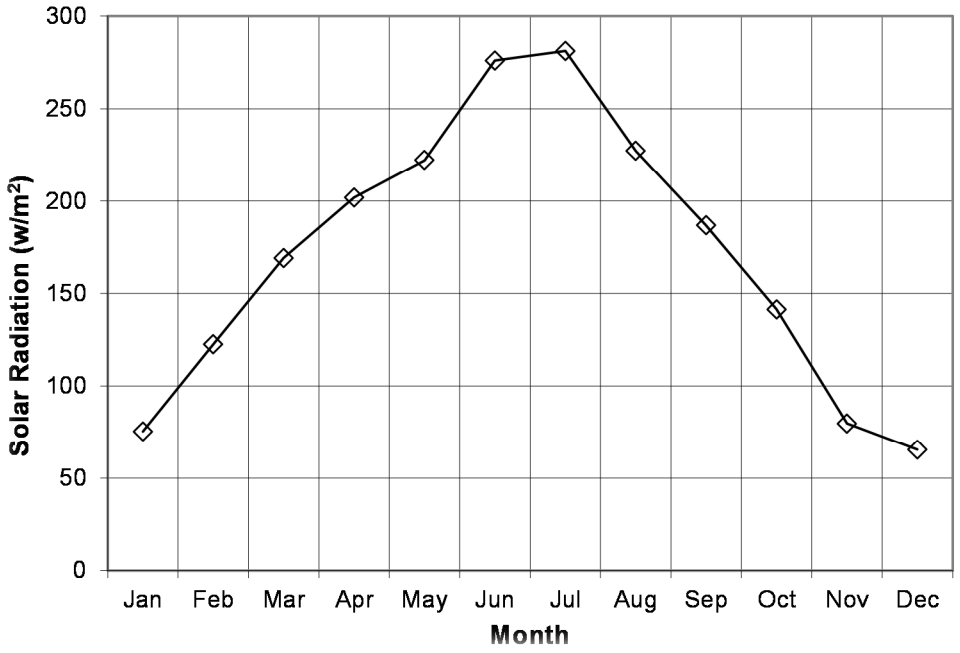

Figure 2.5-28: Ludeman Monthly Evapotranspiriation

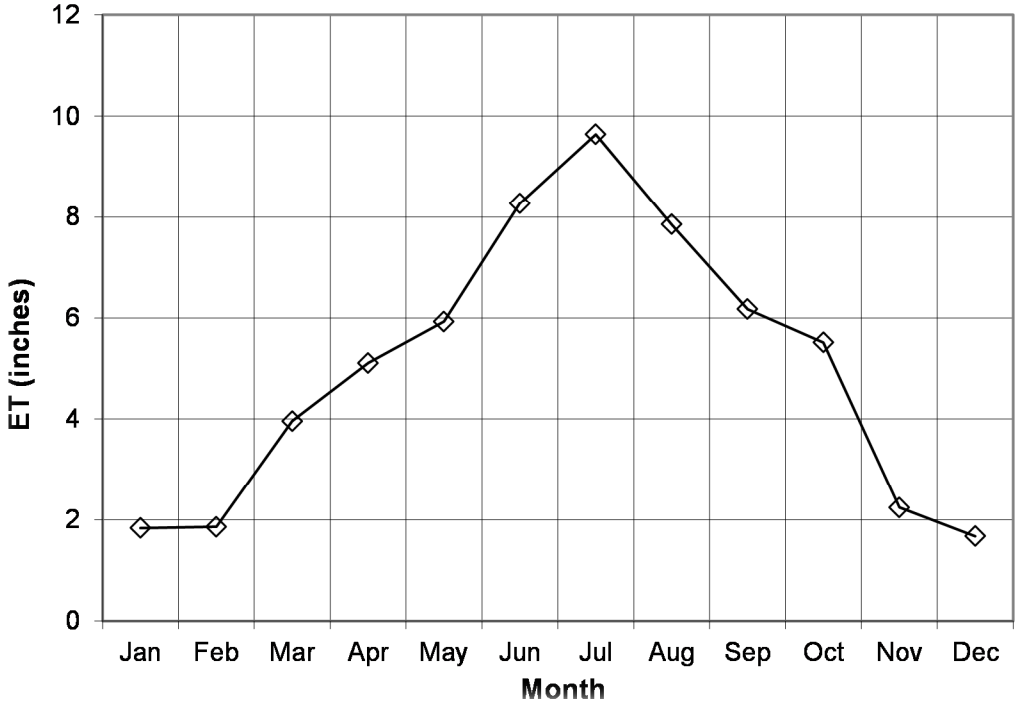

Figure 2.5-29: Ludeman Wind Speed Frequency Distribution

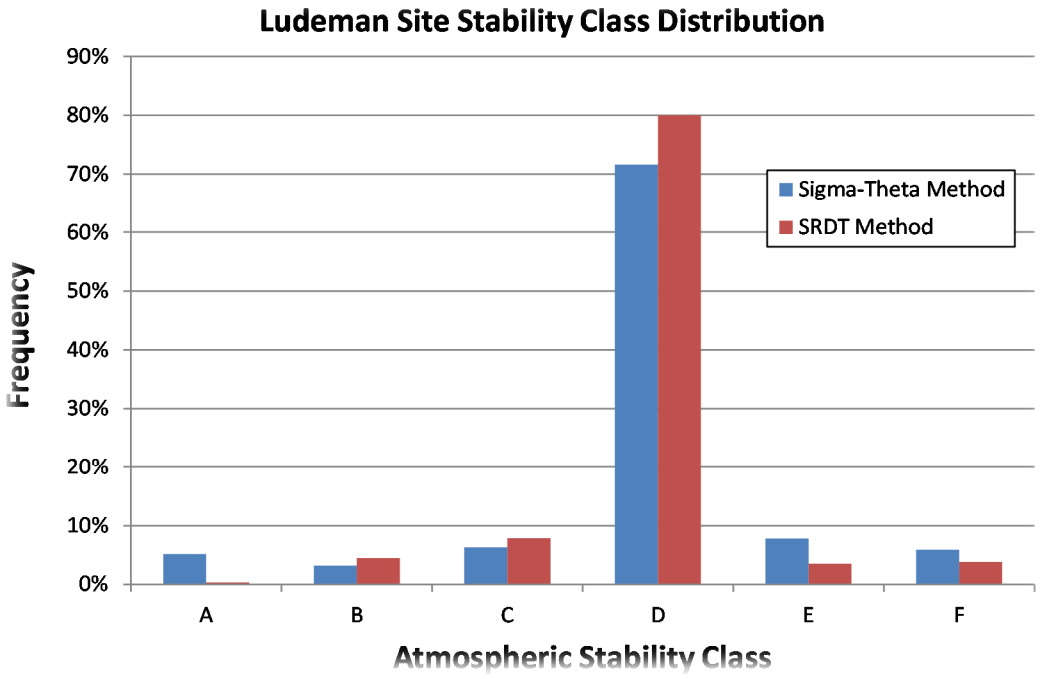

Figure 2.5-30: Casper Long-Term and Short-Term Wind Frequency Distributions

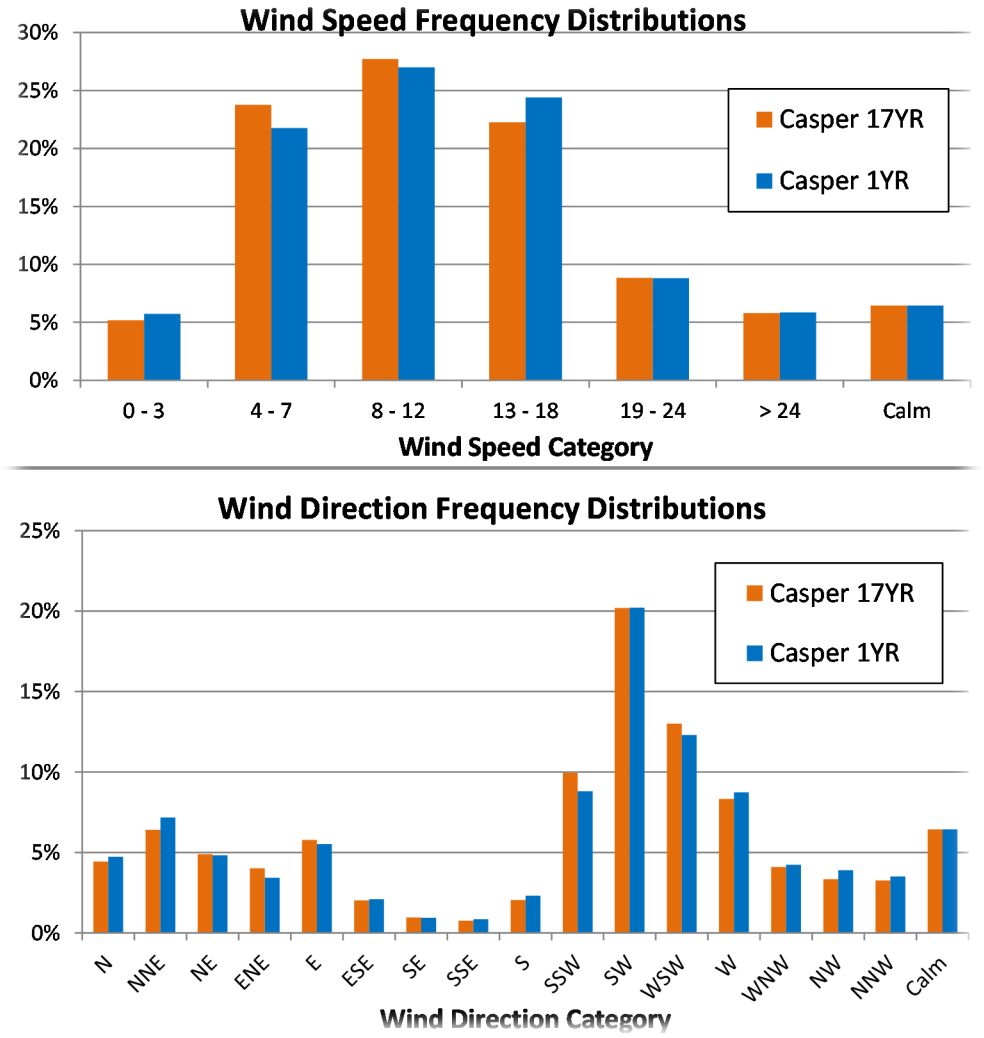

Figure 2.5-31: Casper Long-Term and Short-Term Wind Roses

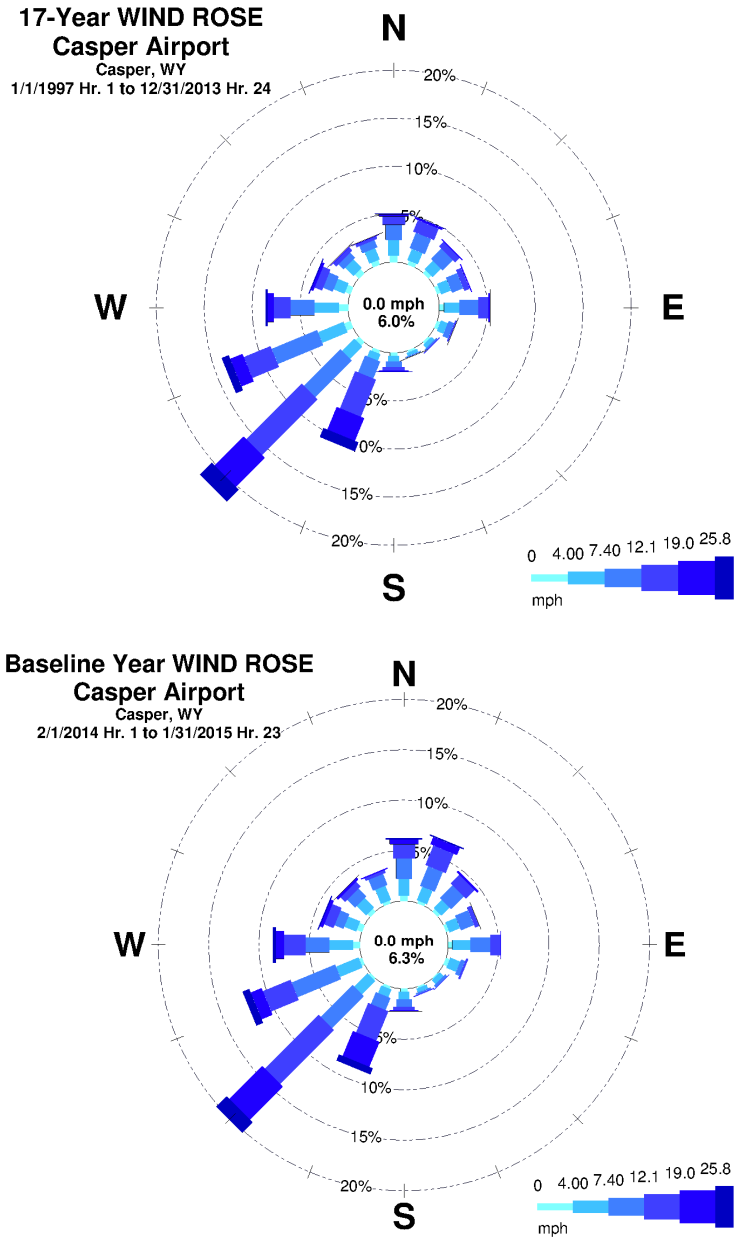

Figure 2.5-32: Casper Long-Term and Short-Term Wind Speed and Direction

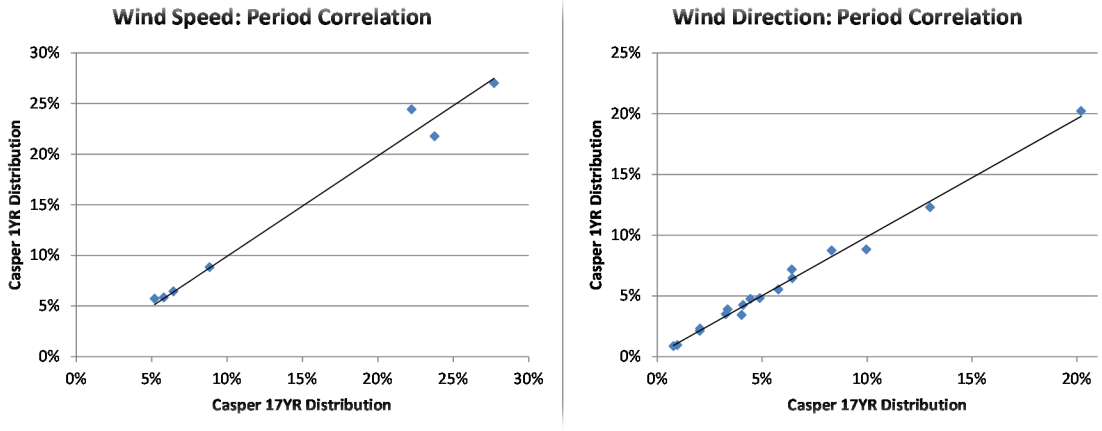

Figure 2.5-33: Casper Long-Term and Short-Term Joint Wind Speed and Direction

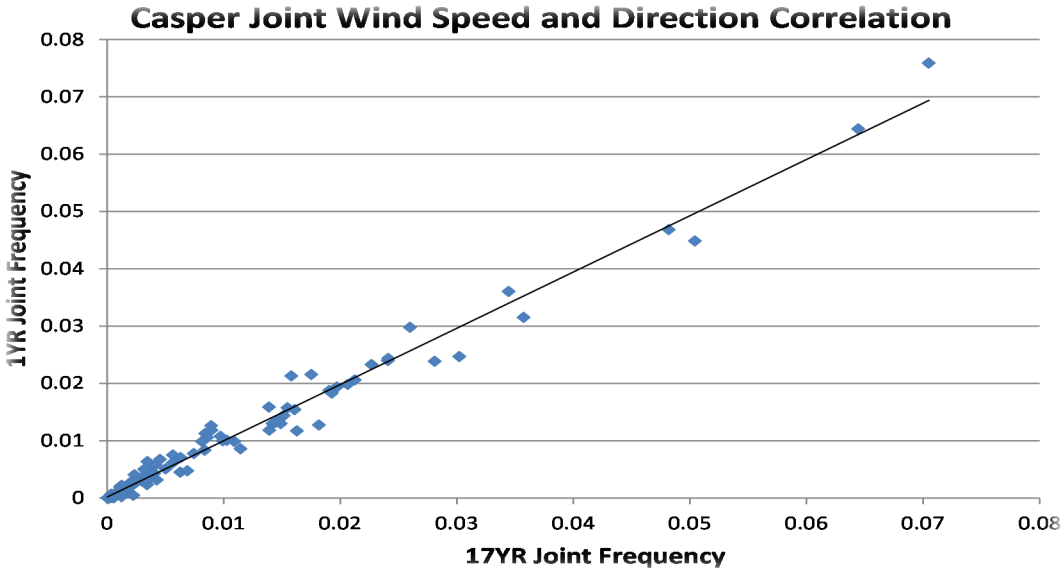

Figure 2.5-34: Casper Short / Long-Term Wind Speed Frequency Distributions

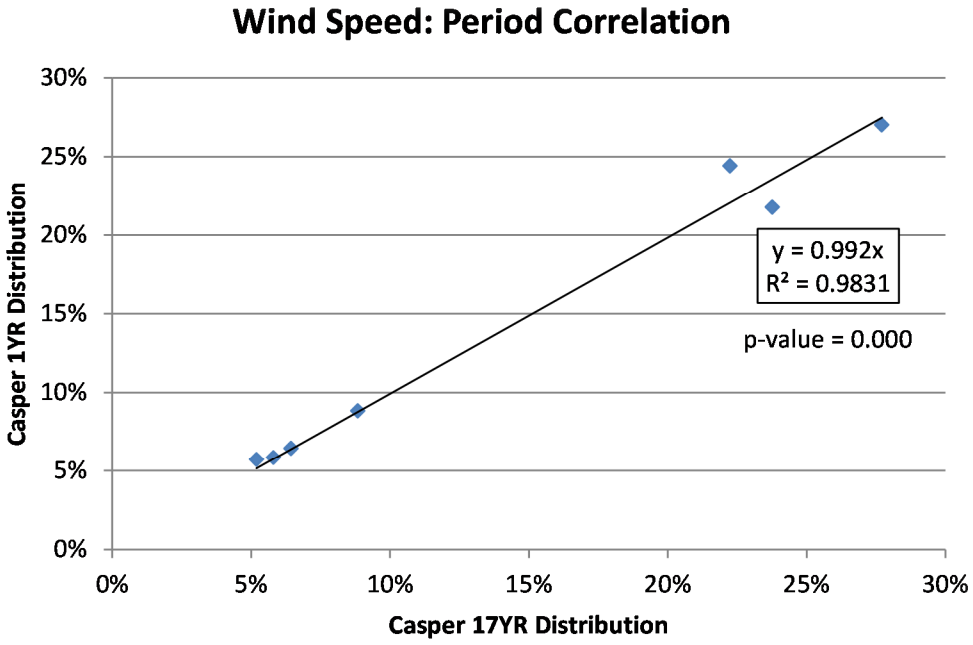

Figure 2.5-35: Casper Short / Long-Term Wind Direction Frequency Distributions

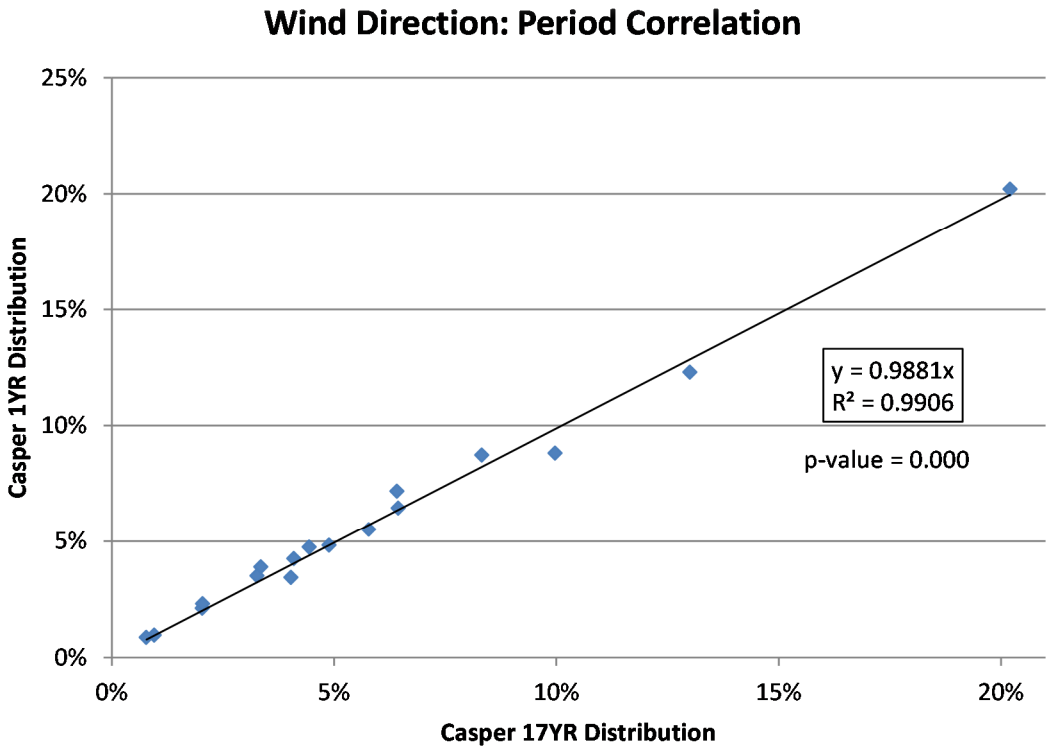

Figure 2.5-36: Casper Short and Long-Term Joint Frequency Distributions

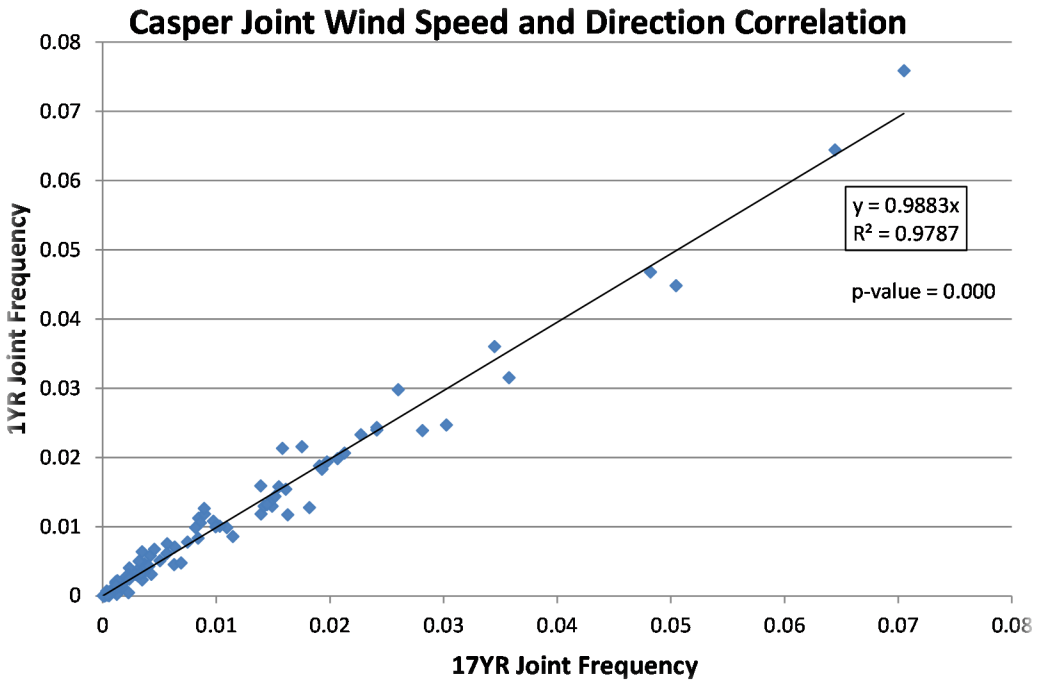

Figure 2.5-37: Douglas Short and Long-Term Joint Frequency Distributions

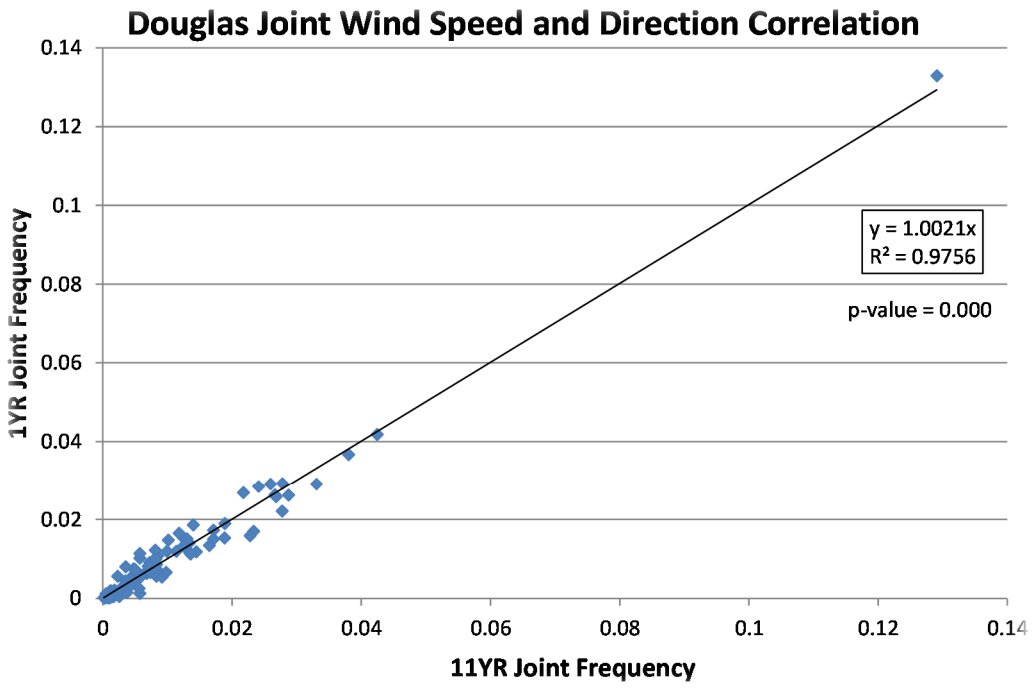

Figure 2.5-38: Douglas and Casper Long-Term Joint Frequency Distributions